Report of Investigation 2018-6

GEOLOGIC MAP OF THE UMIAT–GUBIK AREA, CENTRAL NORTH SLOPE, ALASKA

Trystan M. Herriott, Marwan A. Wartes, Paul L. Decker,
Robert J. Gillis, Diane P. Shellenbaum, Amanda L. Willingham, and David J. Mauel

Published by
STATE OF ALASKA
DEPARTMENT OF NATURAL RESOURCES
DIVISION OF GEOLOGICAL & GEOPHYSICAL SURVEYS
October 2018

Cover. Outcrop of the Nanushuk Formation along the Colville River's north bank at the informally named Colville incision locality. Sandstones of the Nanushuk serve as reservoirs at the Umiat oil field ~20 km to the northeast. Hammer is 31 cm long. Photograph by T.M. Herriott.

GEOLOGIC MAP OF THE UMIAT–GUBIK AREA, CENTRAL NORTH SLOPE, ALASKA

Trystan M. Herriott, Marwan A. Wartes, Paul L. Decker,
Robert J. Gillis, Diane P. Shellenbaum, Amanda L. Willingham, and David J. Mauel

Report of Investigation 2018-6

State of Alaska
Department of Natural Resources
Division of Geological & Geophysical Surveys

STATE OF ALASKA
Bill Walker, Governor

DEPARTMENT OF NATURAL RESOURCES
Andrew T. Mack, Commissioner

DIVISION OF GEOLOGICAL & GEOPHYSICAL SURVEYS
Steve Masterman, State Geologist and Director

Publications produced by the Division of Geological & Geophysical Surveys (DGGS) are available for free download from the DGGS website (dggs.alaska.gov). Publications on hard-copy or digital media can be examined or purchased in the Fairbanks office:

Alaska Division of Geological & Geophysical Surveys
3354 College Rd., Fairbanks, Alaska 99709-3707
Phone: (907) 451-5010 Fax (907) 451-5050
dggspubs@alaska.gov | dggs.alaska.gov

DGGS publications are also available at:
Alaska State Library,
Historical Collections & Talking Book Center
395 Whittier Street
Juneau, Alaska 99811

Alaska Resource Library and Information Services (ARLIS)
3150 C Street, Suite 100
Anchorage, Alaska 99503

Suggested citation:
Herriott, T.M., Wartes, M.A., Decker, P.L., Gillis, R.J., Shellenbaum, D.P., Willingham, A.L., and Maueul, D.J., 2018, Geologic map of the Umiat-Gubik area, central North Slope, Alaska: Alaska Division of Geological & Geophysical Surveys Report of Investigation 2018-6, 55 p., 1 sheet, scale 1:63,360.
http://doi.org/10.14509/30099

Contents

Figures

Appendix 1

Appendix 2

GEOLOGIC MAP OF THE UMIAT–GUBIK AREA, CENTRAL NORTH SLOPE, ALASKA

Trystan M. Herriott,[1] Marwan A. Wartes,[1] Paul L. Decker,[2] Robert J. Gillis,[1] Diane P. Shellenbaum,[2] Amanda L. Willingham,[1] and David J. Mauel[3]

Abstract

A new 1:63,360-scale geologic map of the hydrocarbon-bearing Umiat–Gubik area of the central North Slope, Alaska, spans approximately 2,100 km^2 at the northern extent of the Brooks Range foothills fold-and-thrust belt in the Colville foreland basin. This geologic map was prepared through assimilation of field observations, aerial and satellite imagery, seismic-reflection data, and well logs. Near-surface formation picks were available or derived for most of the area's 24 exploration wells, and two cross sections were constructed along lines of section that are constrained at depth by our interpretations of publicly available two-dimensional seismic data.

The mapped area hosts exposures of Upper Cretaceous strata in the Nanushuk, Seabee, Tuluvak, Schrader Bluff, and Prince Creek Formations, constituting an approximately 2-km-thick succession that crops out discontinuously in the low-relief, tundra-mantled region. This part of the siliciclastic Brookian megasequence stratigraphy comprises principally shallow-marine deposits. Our work benefits from and reflects recent sequence-stratigraphic advances that better constrain how this part of the Colville basin continued to fill by a northeastward prograding clastic wedge during Late Cretaceous time, with the exposed stratigraphy recognized as basin-scale topset units.

A series of east- to east-southeast-trending, km-scale wavelength, gentle folds are mapped in the area. Anticlines are locally breached by thrusts and interpreted to be folded above faulted and penetratively deformed mid-Cretaceous Torok Formation. Undeveloped, sub-commercial (as of this writing) petroleum accumulations occur along doubly plunging anticlinal traps at three long-recognized fields in the map area: Umiat (mostly oil), Gubik (gas), and East Umiat (gas). The Umiat oil field structural culmination is modified by thrust faults that breach the surface, and the East Umiat gas field is associated with a north-dipping back-thrust that is evident in seismic data and cuts across the Upper Cretaceous stratigraphy; thrust faults near the Gubik gas field lie within and below the Torok Formation. Various interpretations have previously been published for some of the area's structures, with important implications for petroleum trap geometries in the gas-prone foothills region. We present new data and interpretations that support the inference of a principal, south-dipping thrust fault that breaches the north limb of Umiat anticline near Umiat. Additionally, a new fracture dataset addresses the previously hypothesized Colville fault. Ultimately, we do not find compelling evidence for a through-going, left-lateral strike-slip fault along the Colville River valley, which extends obliquely across the structural grain of the region. The fracture data are, however, generally consistent with a pure shear model of deformation associated with north–south contraction of the central Brooks Range foothills fold-and-thrust belt.

[1]Alaska Division of Geological & Geophysical Surveys, 3354 College Road, Fairbanks, Alaska 99709-3707
[2]Alaska Division of Oil and Gas, 550 West 7th Avenue, Suite 1100, Anchorage, Alaska 99501-3560
[3]Formerly at Alaska Division of Geological & Geophysical Surveys, 3354 College Road, Fairbanks, Alaska 99709-3707

INTRODUCTION

The Alaska Divisions of Geological & Geophysical Surveys (DGGS) and Oil and Gas (DOG) conducted field studies near Umiat, Alaska (fig. 1), examining the region's Cretaceous stratigraphy and structural geology. Geologic mapping was an integral component of this fieldwork and is the foundation for a new 1:63,360-scale geologic map (sheet 1) that encompasses approximately 2,100 km^2 of the central North Slope in the Brooks Range foothills fold-and-thrust belt (figs. 1 and 2). The North Slope is a large and prolific hydrocarbon province (for example, Bird and Houseknecht, 2011) that hosts the largest oil field in North America at Prudhoe Bay (for example, Magoon, 1994). Umiat is approximately 180 km southwest of Prudhoe Bay (fig. 1) and lies immediately south of the Umiat oil field (Collins, 1958; Molenaar, 1982; Hanks and others, 2014), which was discovered in 1946 and remains undeveloped. Two undeveloped gas fields—Gubik (Robinson, 1958) and East Umiat (for example, Kumar and others, 2002)—also occur in the study area, which is referred to as the Umiat–Gubik area in this paper, and were similarly discovered in the mid-20th century.

The Umiat–Gubik area is characterized by low-relief, treeless hills (fig. 3A) south of the Arctic coastal plain. Locally excellent outcrops (figs. 3B and C) permit observation of Upper Cretaceous Brookian megasequence strata of the dominantly marine Nanushuk, Seabee, Tuluvak, and Schrader Bluff Formations and the chiefly nonmarine Prince Creek Formation (fig. 4). This stratigraphy records a continued phase of primarily northeast-directed, basin axial sedimentation in the Colville foreland basin, which formed and began filling in the Jurassic(?)–Early Cretaceous in response to orogenic thickening in the ancestral Brooks Range (for example, Mull, 1979, 1985; Bird and Molenaar, 1992; Moore and others, 1994; Houseknecht and others, 2009; Bird and Houseknecht, 2011).

Umiat–Gubik and surrounding areas have long been recognized for their importance to understanding the geologic evolution of northern Alaska, with pioneering work led by the U.S. Geological Survey (USGS) (for example, Schrader, 1904; Gryc and others, 1951, 1956; Detterman and others, 1963; Brosgé and Whittington, 1966). Recent investigations by USGS, DGGS, DOG, and university geologists build on the public-domain geologic framework established by these earlier studies and those of the intervening years (for example, Molenaar, 1982; Gryc, 1988), further elucidating the foreland basin's geology (for example, Mull and others, 2003, 2004; Houseknecht and Schenk, 2005; Decker, 2007; Flores and others, 2007a, 2007b; LePain and others, 2009; Flaig, 2010; Flaig and others, 2011, 2013, 2014; Shimer, 2013; Hanks and others, 2014; Sanders, 2014; Shimer and others, 2014, 2016; Wentz, 2014; van der Kolk and others, 2015; van der Kolk, 2016). Additionally, renewed exploration of the Umiat oil field (for example, Lidji, 2015a) and diminished throughput in the Trans-Alaska Pipeline System (for example, Bailey, 2016) have recently underscored the resource potential and economic significance of known petroleum accumulations despite market and technical challenges (for example, Lidji, 2016).

The remainder of this introduction outlines previous geologic mapping in the area and the methods employed during the current study; we also include a brief history of federal exploration programs in the region and general descriptions of the petroleum accumulations in the mapped area. The subsequent sections address the structural geology and stratigraphy of the area, providing a broader context for this work. Sheet 1 presents the 1:63,360-scale Umiat–Gubik area geologic map, a list and correlation of map units, and cross sections A–A' and B–B', which are accompanied by interpreted and non-interpreted, public-domain, two-dimensional seismic profiles.

Previous Geologic Mapping of the Umiat–Gubik Area

Detterman and others (1963) and Brosgé and Whittington (1966) mapped the geology of the Umiat region southeast and northwest of the Colville River, respectively. These 1:125,000-scale

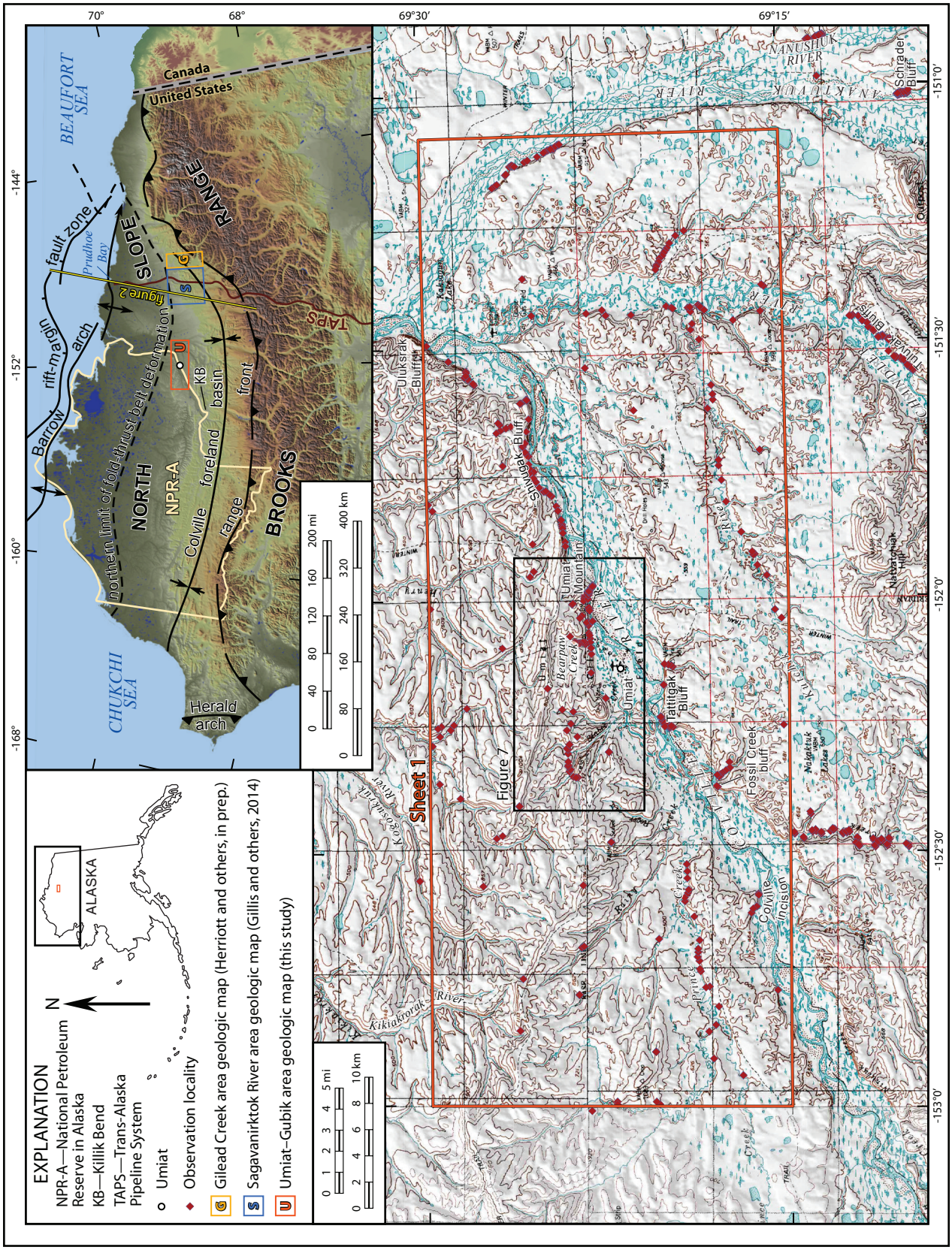

Figure 1. Location map of the Umiat–Gubik area. Detailed field observations were made at ~600 localities during two field seasons in the area. Recent DGGS-led geologic mapping projects in the Sagavanirktok River and Gilead Creek areas are also outlined. Topographic base map from parts of U.S. Geological Survey Umiat and Ikpikpuk River 1:250,000-scale quadrangle maps. Tectonic elements from Decker (2007), which were modified from Grantz and others (1990) and Bird (2001a). Abbreviation: prep.–preparation.

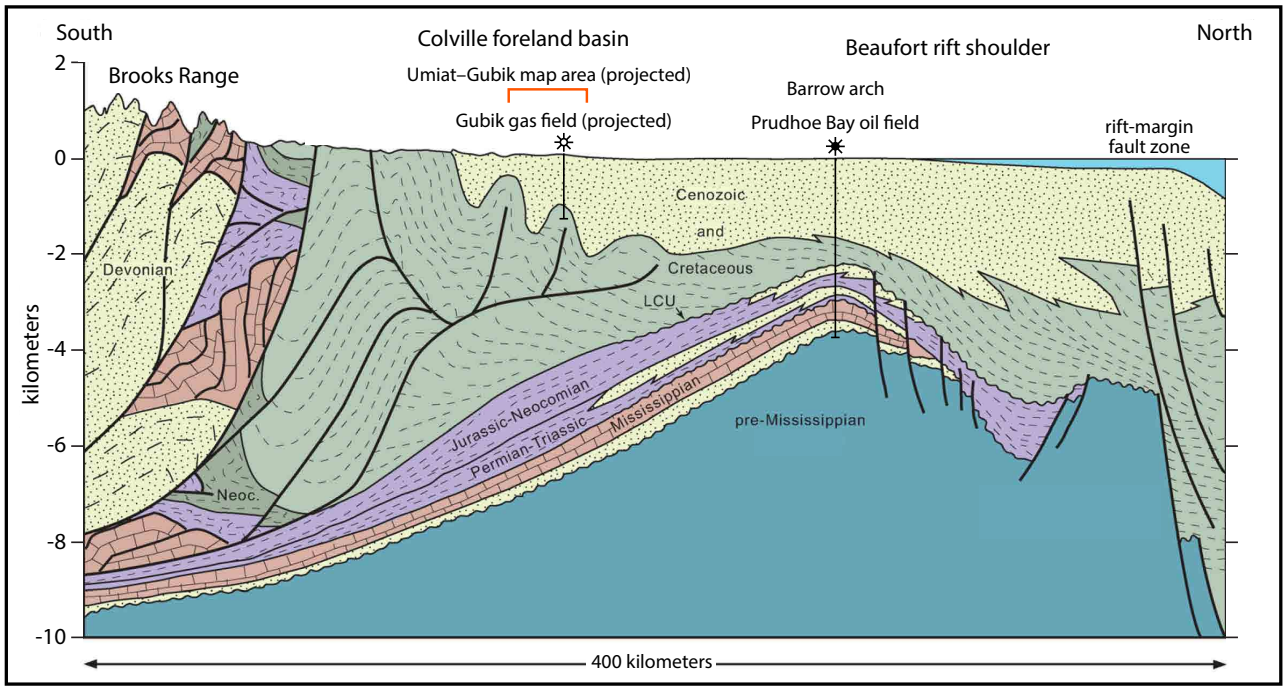

Figure 2. Schematic cross section of the Brooks Range and North Slope from Bird and Houseknecht (2011; modified from Bird and Bader, 1987). See figure 1 for section location. Abbreviation: LCU–Lower Cretaceous unconformity.

geologic maps incorporated extensive stratigraphic and structural studies and early petroleum exploration data (see discussion of Pet-4 program below). Mull and others (2004) subsequently published a 1:250,000-scale geologic map of the Umiat Quadrangle, incorporating the stratigraphic revisions of Mull and others (2003). Application of revised stratigraphic units influenced how the Umiat–Gubik area was mapped and understood, most notably with respect to the Schrader Bluff Formation; we discuss the implications of these revisions below. Mull and others (2004) also reported new structural interpretations for the Umiat Quadrangle, some of which are addressed in this paper.

Present Study–Geologic Mapping and Methods

Field Campaigns and Outcrop Mapping

We conducted two field campaigns in the Umiat–Gubik area, mapping the geology of the Umiat B-5, B-4, B-3, and westernmost part of B-2 quadrangles (1:63,360-scale) on paper topographic maps and approximately 1:60,000-scale aerial photographs (Alaska High Aerial Photography [AHAP] circa 1978–1982). Base camps for these field seasons were set up near the airstrip at Umiat. Field mapping was principally completed with helicopter transportation between widely

Figure 3, opposite page. Photographs exhibiting typical terrain and locally excellent outcrop character of the Umiat–Gubik study area. **A**. View of tundra and low-relief hills in headwaters region of Kikiakrorak River. This landscape hosts limited outcrops and characterizes most of the mapped area. **B**. Oblique aerial view eastward of Shivugak Bluff, exposing Schrader Bluff and Prince Creek Formations. This bluff and others along the Colville River provide the largest outcrops in the study area. Topographic relief of bluff is ~120 m, for sense of scale. **C**. View northward of Schrader Bluff Formation (Barrow Trail Member) along the west bank of the Chandler River. Similar low-relief but excellent cutbank exposures locally occur near rivers and creeks in the map area. Hammer is 31 cm long (see magenta outline). **D**. View southeastward of Schrader Bluff Formation (Barrow Trail Member) rubble-crop and outcrop surrounded by tundra of the upper Kogosukruk River area, with a curvilinear rib of subcrop extending to the left-skyline. This and similar traceable beds are evident along the flanks of Umiat anticline northwest of the Colville River, serving as important constraints to our interpretive geologic mapping. Photographs by T.M. Herriott.


A
B
C
D

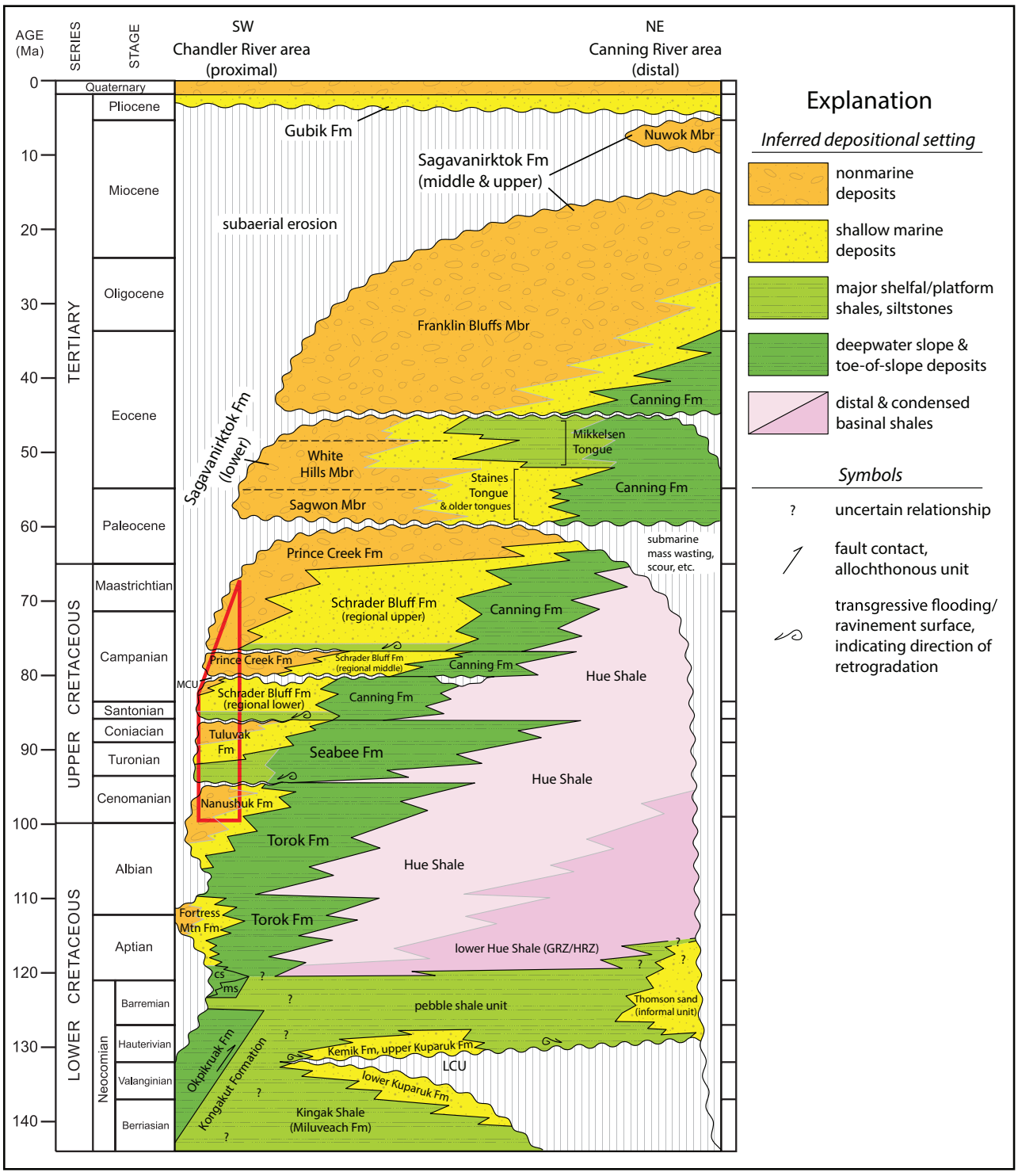

Figure 4. Colville foreland basin chronostratigraphic column from Decker (2010) and Gillis and others (2014) (revised from Mull and others [2003] and Garrity and others [2005]). The stratigraphy that crops out in the Umiat–Gubik area is outlined in red. Parts of three major Brookian depositional cycles occur in the mapped area: Nanushuk–Torok, Tuluvak–Seabee, and Prince Creek–Schrader Bluff–Canning (see text for further discussion). Schrader Bluff Formation members of this study constitute the regional lower part of the formation. Abbreviations: cs–Cobblestone sandstone (informal unit), Fortress Mountain Formation; Fm–Formation; GRZ/HRZ–gamma ray zone/highly radioactive zone; LCU–Lower Cretaceous unconformity; Mbr–Member; MCU–mid-Campanian unconformity (Decker, 2007); ms–manganiferous shale unit (informal unit); Mtn–Mountain.

spaced outcrops. We traversed on foot any laterally extensive or closely spaced outcrops. The Cretaceous stratigraphy commonly crops out along cutbanks of the Anaktuvuk, Chandler, Colville, Kogosukruk, and Kutchik Rivers as well as Prince Creek and several unnamed drainages (figs. 1 and 3C; sheet 1); these exposures typically extended for tens or hundreds of meters. Important km-scale outcrops that expose more than 100 m of stratigraphy occur along the Colville River at Shivugak, Tattitgak, and Uluksrak Bluffs, the south face of Umiat Mountain, and the informally named Colville incision locality (in the sense of LePain and others, 2009) (figs. 1 and 3B; sheet 1). Tundra-mantled uplands constitute most of the field area and are generally devoid of outcrops, but curvilinear trends of subcrop, rubble-crop, and outcrop occur in hilly terrain northwest of the Colville River (fig. 3D) and were mapped on aerial photographs and satellite imagery. We field-checked many of these traceable beds, which serve as excellent stratigraphic markers that are locally correlated to bluff-scale outcrops, rendering high-confidence stratigraphic and structural constraints in otherwise covered areas.

Geologic mapping from the field campaigns was compiled, scanned, georeferenced, and digitized in ESRI ArcGIS ArcMap® software. The mapped surficial geology of sheet 1 is limited to alluvial deposits associated with modern rivers and creeks and simplified from Carter and Galloway (1986). Outcrop distribution is demarcated by map unit polygons with hatched fill (sheet 1). The large, non-hatched swaths of map units that extend across sheet 1 represent the interpreted distribution of the stratigraphy.

Interpretive Geologic Mapping

Limited bedrock exposures occur in the study area, but the distribution of outcrops, character of the deformation, and exploration data permit interpretative geologic mapping of units that generally lie beneath a thin veneer of tundra. Previous workers have published interpretive geologic maps of this region (Detterman and others, 1963; Brosgé and Whittington, 1966; Mull and others, 2004), but sheet 1 is the first geologic map of the Umiat–Gubik area that distinguishes between outcrop and interpreted bedrock geology.

To complete the interpretive mapping, we integrated numerous datasets, including field observations, aerial and satellite imagery, seismic-reflection data, and well logs. Twenty four exploration wells (appendix 1) and numerous seismic surveys have been completed in the Umiat–Gubik area during the past approximately 70 years. We examined well logs and two-dimensional and three-dimensional seismic data (public and confidential), picking formation tops and interpreting structures (fold axial surfaces and fault planes) throughout the mapped area's subsurface.[4] Axial surfaces of km-scale folds evident in the seismic data were projected to their intersections with topography and used to refine axial traces for the folds that were principally identified and/or inferred from field observations. Faults were also interpreted in the seismic data, but were only projected to the surface and mapped on sheet 1 where they cut across the shallowest resolved intervals of the seismic data (typically several hundred meters below the surface). In areas of structural complexity where three-dimensional seismic data were available (for example, the Umiat oil field) we interpreted dip-parallel seismic sections at hectometer-scale spacing. All structures that were identified with, or were better located by, seismic-reflection data are plotted in magenta on sheet 1.

The seismic data do not permit identification of near-surface stratigraphic units, although the stratigraphy identified at greater depths provided important constraints. In mapping the interpreted geologic map unit contacts, we utilized the outcrop mapping described above, bedding orientation data (this study), structural mapping (Brosgé and Whittington, 1966; Molenaar, 1982; Kumar and others, 2002; this study), and known stratigraphic thicknesses (Collins, 1958; Robinson, 1958; Detterman

[4]Seismic and well data from qualifying industry exploration conducted within the study area since 2007 were released by the Alaska Department of Natural Resources in 2017 and 2018, including three-dimensional seismic surveys at the Umiat and Gubik fields. Contact DGGS or DOG for further information regarding these now publicly available tax-credit data.

and others, 1963; Brosgé and Whittington, 1966; DGGS, unpublished data). We also employed uppermost formation picks made by Kenneth J. Bird (U.S. Geological Survey, written communication, 2010) and publicly available well completion reports from the Alaska Oil and Gas Conservation Commission (AOGCC), Collins (1958), and Robinson (1958) (appendix 1). The interpretive mapping was an iterative process, refined and corroborated by examination of the multiple data sources noted here. However, the interpretive contacts are generally marked as inferred (short-dashed lines) except where they are constrained by nearby outcrops or subcrop, where they are designated as approximately located (long-dashed lines).

Note that local seismic data interpreted in this study were converted from travel time to approximate depth for illustrative purposes using a simple velocity field interpolated from wells tied to the seismic data. Seabee Test No. 1 and Gubik No. 4 wells' time–depth relations significantly influenced the depth conversions. More rigorous depth conversion techniques would be appropriate for planning wells or detailed reservoir analyses.

Cross Sections

Cross sections A–A' and B–B' (sheet 1) were similarly constructed though the integration of our field geologic mapping and subsurface data. The subsurface geology of A–A' is based on our interpretation of the public-domain, two-dimensional seismic line U8-78 (Triezenberg and others, 2016); the line of section is coincident with the seismic line (fig. 5). The near-surface seismic character of U8-78 does not permit identification of formation tops above the Nanushuk Formation to the south, the Torok Formation near the Umiat anticline's crest, and the Seabee Formation to the north. Geologic mapping and known stratigraphic thicknesses were compared to and combined with the seismic interpretation to complete A–A'. A similar approach was employed for B–B', which in the subsurface is based on the public-domain, two-dimensional seismic line 720-80 (Triezenberg and others, 2016); the line of section nearly coincides with the seismic line (fig. 5). The Tuluvak Formation top is the uppermost formation pick for most of 720-80 along B–B', with none of the Schrader Bluff Formation members readily identifiable in the seismic data. The near-surface interpretation for the Rogers Creek, Barrow Trail, and Sentinel Hill Members (Schrader Bluff Formation) and the Prince Creek Formation of B–B' is based on geologic mapping and stratigraphic thickness constraints (see below). Non-interpreted and line-drawing interpretations for the two seismic sections are presented on sheet 1. The cross sections are not line or area balanced.

Overview of Petroleum Geology in the Umiat–Gubik and Surrounding Areas

Documentation of oil seeps along the northern coast of Alaska dates to the early 20th century (Brooks, 1916; Leffingwell, 1919), which contributed to the establishment of Naval Petroleum Reserve No. 4 (NPR-4) in 1923 (see NPR-A on fig. 1). Early geologic reconnaissance of the petroleum reserve was conducted by the USGS during 1923–1926 (Smith and Mertie, 1930). An initial phase of exploration in NPR-4 was led by the U.S. Navy in collaboration with the USGS, beginning in 1944 as a strategic response to the energy needs of World War II (Reed, 1958). During this program, which was referred to as Pet-4, the USGS completed regional geologic studies in and beyond NPR-4, including the geologic mapping of Detterman and others (1963) and Brosgé and Whittington (1966). The work also included an extensive drilling program and geophysical surveys. Three oil fields and five gas fields were discovered, including the Umiat (dominantly oil) and Gubik (gas) fields that lie in the current map area, and Pet-4 concluded in 1953. Subsequent industry-led drilling in the mid-1960s led to the discovery of a third petroleum accumulation in the mapped area, the East Umiat gas field (see Molenaar, 1982).

A second federal exploration program in NPR-4, renamed the National Petroleum Reserve in Alaska (NPR-A) in 1977, was conducted from 1974 through 1981. The program included drilling 28 test wells. One of these wells, Seabee Test No.

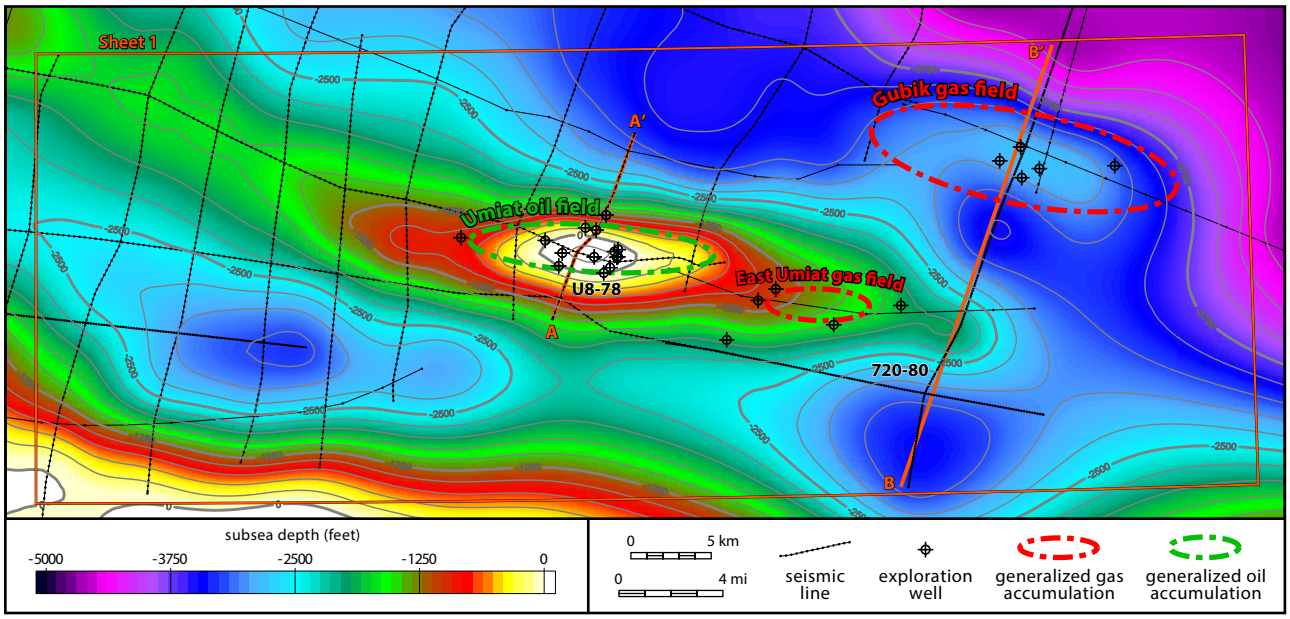

Figure 5. Depth structure map of Umiat–Gubik map area based on publicly available seismic data grid shown in thin black lines with shot points. Reference datum is top Nanushuk Formation. Note that oil and gas field outlines are generalized (see also Division of Oil and Gas, 2008). See figure 1 for index map.

1 (appendix 1), was drilled at the Umiat oil field, penetrated Lower Cretaceous Brookian intervals (for example, Molenaar, 1982) and had numerous oil and gas shows (sheet 1: cross section A–A', Umiat oil field detail). Similar to the Pet-4 phase of exploration, extensive geologic and geophysical surveys were conducted throughout and beyond NPR-A. USGS Professional Paper 1399 (Gryc, 1988) presented the geologic and geophysical work of this latest government-led exploration program in NPR-A. Extensive summaries of the U.S. Navy and USGS work in NPR-4/NPR-A are presented by Smith and Mertie (1930), Reed (1958), Bird (1981), and Schindler (1988).

Hydrocarbon Accumulations in the Mapped Area

The region's Mesozoic stratigraphy hosts numerous petroleum source rocks, including the Shublik Formation, Kingak Shale, pebble shale unit, Hue Shale, and Torok Formation (for example, Magoon and Bird, 1985; Magoon, 1994; Houseknecht and Bird, 2006). All of these units lie in the Umiat–Gubik area subsurface (see sheet 1 cross sections). Petroleum generation, migration, and trapping in the central Brooks Range fold-and-thrust belt is generally interpreted to be tied to tectonic burial, sedimentation, and deformation of the Brooks Range and Colville foreland basin during mid-Cretaceous to Paleocene time (~120–60 Ma) (for example, Bird and Houseknecht, 2011). Many of the structural traps in the central foothills are km-scale anticlines, locally modified by thrust faults, that likely formed at approximately 60 Ma (for example, O'Sullivan and others, 1997; Moore and others, 2004). Petroleum systems modeling of the central fold-and-thrust belt suggests a main phase of mid-Cretaceous oil generation followed by additional Late Cretaceous burial and Paleocene structural trap formation, rendering a generally gas-prone region (see Bird and Houseknecht, 2011). We refer the interested reader to Magoon (1994), Magoon and others (2003), Moore and others (2004), Houseknecht and Bird (2006), Peters and others (2006), and Bird and Houseknecht (2011) for further information regarding petroleum systems evolution in northern Alaska.

The Umiat–Gubik area petroleum accumulations (fig. 5) occur along doubly plunging, gently folded (fig. 6) anticlinal traps; hydrocarbon accu-

Figure 6. Oblique aerial photographs of gentle (limbs dip ≤10°), km-scale wavelength folds that are typical of the map area. **A**. View westward of the east-south-east-trending (~115°) Kutchik syncline at Shivugak Bluff. Fold limbs at left and right of photograph are the north limb of the Umiat anticline and south limb of the Gubik anticline, respectively. Fold axis is near center of photograph. Topographic relief of bluff at right of photograph is ~120 m; field of view is more than 8 km along the Colville River, for sense of scale. **B**. View westward of the west-plunging end of the east-trending (~095°) Gubik anticline, with the south and north limbs cropping out at easternmost Shivugak Bluff (see right of A) and southwesternmost Uluksrak Bluff, respectively. Fold axis is near center of photograph. Field of view between the two bluffs is ~3.75 km, for sense of scale. Photographs by T.M. Herriott.

mulations are in the Nanushuk Formation and younger Cretaceous stratigraphy that is folded over structurally thickened Torok Formation. Both the Umiat and East Umiat fields are modified by thrust faults (Brosgé and Whittington, 1966; Molenaar, 1982; Kumar and others, 2002; this study).

Umiat Oil Field

The Umiat oil field (fig. 5) was the first oil accumulation discovered on the North Slope. The field lies along a faulted extent of the Umiat anticline north of Umiat (sheet 1). Eleven wells were drilled into Nanushuk Formation reservoir targets during 1945–1952, with discovery of the oil field in Umiat Test No. 3 in 1946 (Collins, 1958; Molenaar, 1982; Bird and Bader, 1987). As noted above, an additional well (Seabee Test No. 1) was drilled several decades after the oil field had been discovered. Renewed industry exploration of the Umiat field has been ongoing during the past decade, with the acquisition of a three-dimensional seismic survey in 2008 (Watt and others, 2010) and new wells drilled during 2013 (Umiat No. 18) and 2014 (Umiat No. 23H) (see Lidji, 2015a, 2016; appendix 1). Estimates of recoverable oil resources discovered at the Umiat field range between many tens and several hundred million barrels (see Lidji, 2012, 2015b), with a commonly cited value of 70 million barrels (Molenaar, 1982). Geologic modeling by Hanks and others (2014) indicated 1.52 billion barrels of original oil in place at the Umiat field, with 99 billion cubic feet of associated gas, and these authors presented a reservoir simulation analysis that suggested an oil recovery efficiency of 12–15% through 50 years of modeled production. The oil source rock in the Umiat accumulation is probably the lowermost Brookian gamma ray zone (GRZ)/highly radioactive zone (HRZ) of the Hue Shale (Magoon and others, 2003; fig. 4). The main oil reservoirs in the Umiat field are Albian delta front and shoreface sandstones (Molenaar, 1982; Hanks and others, 2014; Shimer and others, 2014) of the Nanushuk Formation (the Grandstand Formation of former usage) (Collins, 1958; Molenaar, 1982). Hanks and others (2014) reported an API (American Petroleum Institute) gravity of 37° for Umiat oil, and the reservoirs are mostly in permafrost. The locally doubly plunging anticline provides, in combination with thrust truncation (sheet 1: cross section A–A', Umiat oil field detail), structural closure over an area of approximately 7,500 acres (Kumar and others, 2002).

Oil shows and oil produced on tests suggest that the Umiat field oil column extends above the main reservoir sandstones (transitional marine and nonmarine Nanushuk Formation interval formerly recognized as upper Grandstand Formation) into lower-reservoir-quality sandstones (fully marine Nanushuk Formation interval formerly recognized as Ninuluk Formation).[5] As noted by Molenaar (1982), there is insufficient information from the wells to define a precise oil–water contact, and there is at least local evidence for reservoir compartmentalization and separate fluid contacts in upper and lower Grandstand sandstones. Molenaar (1982) estimated the oil–water contact in the upper Grandstand on the southern flank of the structure at about -650 feet subsea, between the Umiat Test No. 6 (oil productive) and the Umiat Test No. 7 (wet) wells. This is broadly consistent with the bottom of persistent oil shows and resistivity log response observed in the Seabee Test No. 1 well at -440 feet subsea (see sheet 1: cross section A–A', Umiat oil field detail). The top of the upper Grandstand reservoir horizon is mapped (Brosgé and Whittington, 1966; Watt and others, 2010) as having a crestal depth of approximately +250 feet subsea (that is to say, 250 feet above sea level), yielding a potentially productive oil column in the main reservoir interval of about 690–700 feet. This main reservoir interval is the lower part of the thicker, generalized oil column of cross section A–A' (sheet 1: Umiat oil field detail), which includes the Ninuluk interval noted above.

Gubik Gas Field

The Gubik gas field (fig. 5) was discovered in 1951 when two wells (Gubik Test Nos. 1 and 2; appendix 1) were drilled following delineation

[5] See Mull and others (2003) for former and current Nanushuk Formation stratigraphic nomenclature.

of the Gubik anticline (fig. 6B and sheet 1) by geologic and geophysical studies during 1945–1950 (Robinson, 1958; Bird and Bader, 1987). One additional well was drilled on the Gubik anticline during industry activity in 1963, and two industry wells were completed in 2008 and 2009 (appendix 1). Recoverable gas resources at Gubik are estimated at 600 billion cubic feet (Kornbrath and others, 1997) and hosted largely by the Tuluvak Formation (Robinson, 1958; Mull and others, 2003). This gas may be sourced from the gas-prone, terrestrial kerogen-rich Torok Formation, as has been proposed for the Aupuk gas seep southwest of the current study area (Decker and Wartes, 2008). The doubly plunging anticline provides structural closure over an area of approximately 20,000 acres and 800 vertical feet (Kumar and others, 2002; see also Robinson, 1958).

East Umiat Gas Field

The East Umiat gas field (fig. 5) was discovered during industry drilling in the winter of 1963–1964 (Molenaar, 1982; Bird and Bader, 1987). Three additional wells were completed in the following decade and a fifth well was drilled in 2008–2009 (appendix 1). The field lies along the Umiat anticline east-southeast of the Colville River, and 4 billion cubic feet of recoverable gas resources were reported by Kornbrath and others (1997). Gas in the East Umiat field is hosted in numerous Nanushuk Formation intervals (Bird, 1988a; Kumar and others, 2002) and, similar to the Gubik gas field, may be sourced from the gas-prone Torok Formation. The locally doubly plunging anticline provides structural closure over an area of approximately 5,000 acres and less than 100 vertical feet (Kumar and others, 2002).

STRUCTURAL GEOLOGY

Regional Context–Brookian Orogenesis

Structural, stratigraphic, and thermochronologic studies in northern Alaska indicate a long-lived, multi-phase Brooks Range orogeny that spans the past approximately 175 million years (for example, Mull, 1982; Mayfield and others, 1988; Bird and Molenaar, 1992; Moore and others, 1994, 2004; Blythe and others, 1996; Cole and others, 1997; Mull and others, 1997; O'Sullivan and others, 1997; Vogl and others, 2002). Middle Jurassic to Early Cretaceous contraction emplaced a series of thin-skinned allochthons that were progressively stacked in sequence from south to north along orogen-scale thrust faults, collapsing a south-facing passive margin that rifted to the north and collided with an oceanic island arc to the south (for example, Mull, 1982; Mayfield and others, 1988; Moore and others, 1994; Wallace, 2008). This thick succession of allochthons resulted in hundreds of kilometers of shortening, loading the lithosphere and driving subsidence in the Colville foreland basin to the north (see reviews by Bird and Molenaar, 1992; Moore and others, 1994). Cole and others (1997) reported that maximum tectonic loading was achieved in the Barremian. Uplift and extension exhumed part of the orogen's hinterland along south-dipping normal faults in the southern Brooks Range (Miller and Hudson, 1991) during mid-Cretaceous time (~113–95 Ma; Blythe and others, 1996; Vogl and others, 2002; see also Turner and others, 1979), although contemporaneous contraction may have continued to the north (Oldow and others, 1987; Till, 1992; Moore and others, 1994; Till and Snee, 1995; Cole and others, 1997). This episode of mid-Cretaceous uplift likely marked the first subaerial exposure of the Brooks Range orogen (Wallace, 2008). The ancestral Brooks Range and regions farther west provided prolific source areas for large volumes of Aptian(?)–Cenomanian Nanushuk–Torok sediment that spilled north and east into the underfilled foreland basin (for example, Molenaar, 1985, 1988; Bird and Molenaar, 1992; Houseknecht and Schenk 2001; Houseknecht and others, 2009; Bird and Houseknecht, 2011). Post-Nanushuk–Torok Upper Cretaceous units accumulated during a period of apparent tectonic quiescence, which was followed by a later phase of renewed Brookian contraction at approximately 60 Ma (Blythe and others, 1996; O'Sullivan and others, 1997; Mull and others, 1997; Moore and others, 2004). This Paleocene event propagated the fold-and-thrust

belt into the foreland basin, including the Umiat–Gubik study area, rendering km-scale uplift of the Upper Cretaceous stratigraphy (Blythe and others, 1996; O'Sullivan, 1996; Cole and others, 1997; O'Sullivan and others, 1997; Gillis and others, 2014). Episodic shortening and uplift continued in the east-central and northeastern Brooks Range during Paleogene time (for example, O'Sullivan, 1996; O'Sullivan and others, 1993, 1997, 1998; O'Sullivan and Wallace, 2002), and deformation in northeasternmost Alaska and outboard Beaufort Shelf remains ongoing today (Grantz and others, 1983, 1990; Moore and Box, 2016).

Umiat–Gubik Area Structure

The Umiat–Gubik study area lies in the northern part of the central Brooks Range foothills fold-and-thrust belt (figs. 1 and 2). We highlight two key aspects of the Brookian orogeny that bear directly on the structural geology of the Umiat–Gubik area. 1) Significant subsidence of the foredeep and its marked filling by Torok–Nanushuk depositional systems (for example, Molenaar, 1988; Houseknecht and Schenk, 2001; Houseknecht and others, 2009; LePain and others, 2009) rendered a mechanical stratigraphy comprising the approximately 3-km-thick, mud-prone Torok overlain by the thinner, approximately 300-m-thick, sand-prone Nanushuk (thicknesses after Molenaar, 1982). This stratigraphic juxtaposition of mechanically weak (Torok) and rigid (Nanushuk) units strongly influenced the character of deformation in the foothills fold-and-thrust belt (for example, Moore and others, 2004; Wallace, 2008; Mull and others, 2009; Sanders, 2014). 2) The Upper Cretaceous stratigraphy of the study area was deformed during the approximately 60 Ma cooling event (see references above), with penetrative and thrust-related structural thickening in the Torok Formation and gentle detachment folding and thrusting of the overlying Nanushuk and younger formations (for example, Molenaar, 1982; Kirschner and Rycerski, 1988; Mull and others, 2004; Sanders, 2014; this study). These events and their timing were also critical to generation and trapping of oil and gas in the region (for example, Moore and others, 2004).

Five large (km-scale wavelength) folds are mapped in the study area (south to north): Fossil Creek anticline, Prince Creek syncline, Umiat anticline, Kutchik syncline (fig. 6A), and Gubik anticline (fig. 6B) (sheet 1; Detterman and others, 1963; Brosgé and Whittington, 1966; Mull and others, 2004). Structural relief across this fold train diminishes to the north and east (fig. 5), a trend that is reflected in the distribution of generally younger strata to the northeast. Only minimal deformation of the Upper Cretaceous stratigraphy is evident north of the study area, where the northern limit of deformation is delineated (for example, Mull and others, 2004; figs. 1 and 2). Folds in the map area generally plunge to the east-southeast, although many of these structures are locally doubly plunging and form traps at the Umiat, East Umiat, and Gubik hydrocarbon accumulations discussed above. Axial surfaces are chiefly upright or dip very steeply; anticlinal crests are locally truncated by north- or south-dipping thrust faults (sheet 1). Folds are gentle, with limbs principally dipping less than 10 degrees (fig. 6).

Anticlines in the area are recognized as detachment folds that are commonly thrust-modified (for example, Molenaar, 1982; Sanders, 2014). Consistent with the work by Sanders (2014), our seismic-based cross sections indicate a mid-Torok interval prone to forming imbricate fault arrays and duplexes over a probable lower Torok detachment interval, with north-dipping, passive-roof thrusts locally ramping into or entirely truncating an upper Torok interval (sheet 1: cross sections A–A' and B–B'). Mull and others (2004, 2005) highlighted that some anticlines of the central Brooks Range foothills fold-and-thrust belt are cut by north-dipping, breaching back-thrusts, a structural style that may be even more common near the range front to the south (for example, Mull and others, 2009); we interpret such a case near the East Umiat gas field (sheet 1: cross section B–B' at Umiat anticline). The Gubik anticline is not faulted at the surface, but our interpretation of seismic-reflection data indicates a back-thrust terminates in the upper Torok below the Gubik gas field (sheet 1: cross section B–B'). Our examination of seismic data that image

the Fossil Creek anticline near the southwest bank of the Colville River suggests a locally complex structure with two anticline crests juxtaposed by a south-dipping thrust fault (sheet 1). Future investigations west and south of the study area may shed further light on the Fossil Creek anticline's fault–fold association.

The following sections address the Umiat oil field area structural geology and the potential for a regional-scale, left-lateral strike-slip fault along the Colville River corridor.[6] We review previous studies relevant to these areas and present new work that further constrains the structural relations, which have implications for the style of deformation and potential trap geometries in the gas-prone foothills fold-and-thrust belt.

Umiat Oil Field Structure

Faulting associated with the Umiat oil field has long been recognized, with seismic and well data from the 1940s revealing a fault–fold association (Collins, 1958; Brosgé and Whittington, 1966). North of the fold's axial trace, Brosgé and Whittington (1966) mapped a series of faults in a zone that is generally several hundred meters wide and associated with a prominent topographic lineament (fig. 7) defined by steeply north-dipping sandstone beds. The steep dips are anomalous, as the fold limbs chiefly dip gently in areas north and south of the lineament (sheet 1). Brosgé and Whittington (1966) also reported offset (downthrown to north ~50 feet) of bench-forming Nanushuk Formation outcrops east of Bearpaw Creek (see sheet 1 and fig. 7) and remarked that this is the only "direct evidence of faulting" at the surface in their mapped fault zone. These authors ultimately described and portrayed a fault zone comprising a complex of south-dipping thrust faults rooted in the Torok, with up to 2,000 feet of stratigraphic separation across the zone. Molenaar (1982) built on the earlier work of Brosgé and Whittington (1966) and attributed the thrust-faulted Umiat anticline to detachment folding of the Nanushuk and Upper Cretaceous stratigraphy over faulted and penetratively deformed Torok. Similar to the previous geologic mapping of the area, Mull and others (2004) recognized structural significance in the topographic lineament, but rather mapped the feature as the breaching trace of a north-dipping back-thrust, noting that back-thrusts in the region commonly occur where Nanushuk Formation crops out near fold crests.

Our mapping of the Umiat anticline also documents that the limbs principally dip gently, with moderately to steeply dipping bedding near the topographic lineament (fig. 7 and sheet 1). We completed foot traverses along the approximately 15-km-long lineament, which we map as a north-dipping panel of Tuluvak Formation in the north limb of the anticline. The map pattern identifies juxtaposition of stratigraphic units across the lineament of the same formation, or, more commonly, a younger formation to the north, with the greatest stratigraphic separation near Bearpaw Creek and diminishing separation to the east and west (fig. 7 and sheet 1; compare with Brosgé and Whittington, 1966; Molenaar, 1982; Hanks and others, 2014).

We observed bedrock rubble with slickensides at two localities (11BG254 and near 11BG263) near the western end of the lineament, and two additional nearby locations (11BG269 and 11BG270) host faults in small outcrops (fig. 7). Numerous slip planes at these latter two localities exhibited grooves, shear steps defined by fibrous crystal growth, and serrated asperities produced by secondary shear steps on non-mineralized planes; these faults dominantly dip moderately to steeply to the north and south, with one fault dipping steeply eastward. Kinematic indicators at these outcrops principally suggest normal slip, with some of the fault planes closely paralleling or coinciding with bedding planes. Farther east, the Bearpaw Creek area reveals steeply dipping Tuluvak Formation strata defining the lineament and subhorizontal to gently dipping benches

[6] Note that the right-lateral strike-slip fault that we map along the Colville River near Umiat (see tear fault(?) of sheet 1) is of limited extent (<5 km) and is not an equivalent to the regional-scale, left-lateral strike-slip fault (that is to say, the Colville fault of Mull and others, 2004, 2005) discussed below.

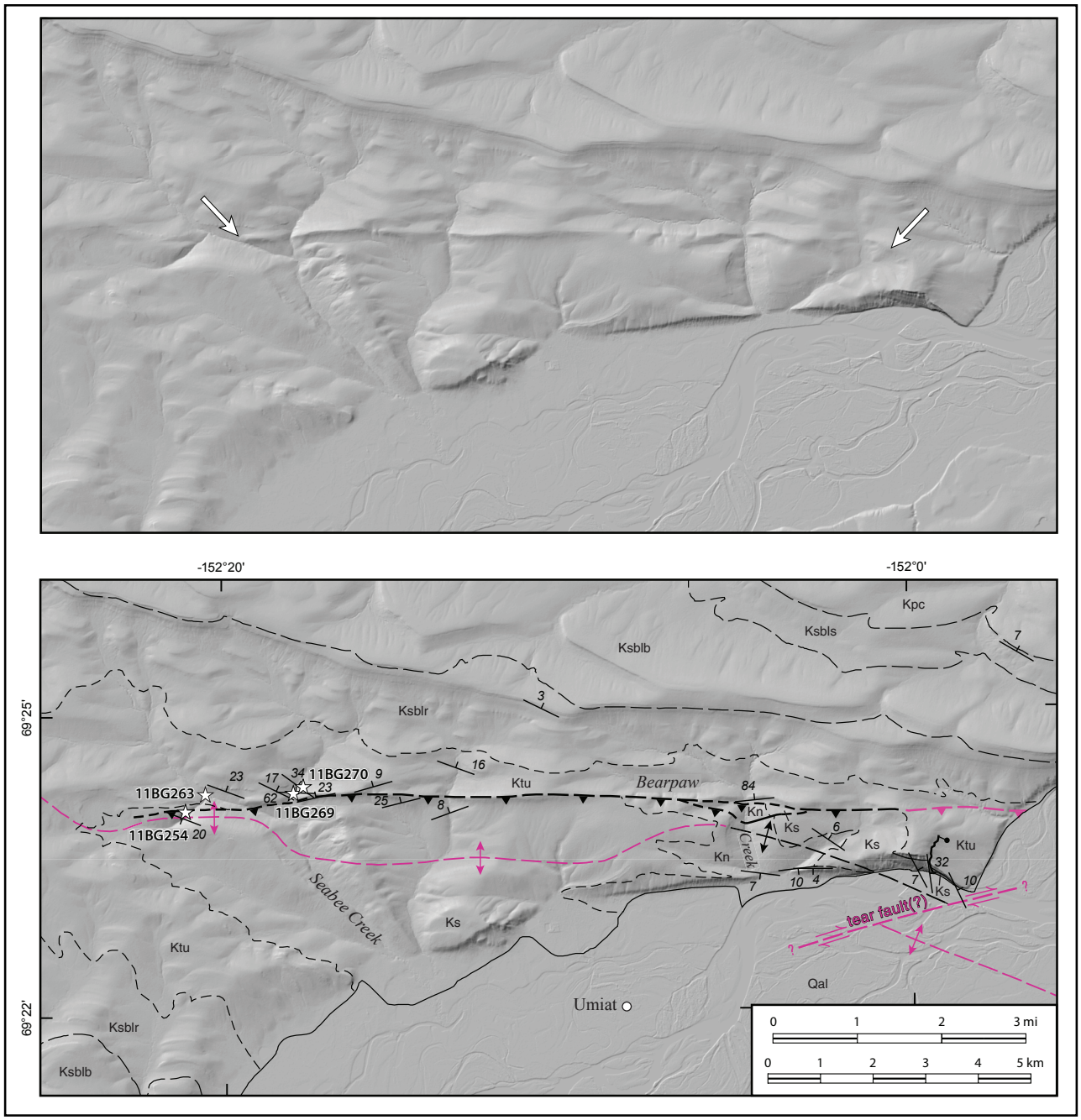

Figure 7. Interferometric synthetic aperture radar (IFSAR)-based shaded-relief map of Umiat anticline near Umiat. Note the prominent topographic lineament (see between arrows in A) and field localities (see stars in B) discussed in text. Geologic linework and symbols are from sheet 1; see figure 1 for index map.

of Nanushuk Formation cropping out several hundred meters to the south (sheet 1 and fig. 7); we do not map Seabee Formation along the creek (compare with Mull and others, 2004). Additionally, the bench-forming Nanushuk outcrops are distinctly offset (downthrown to north) immediately east of Bearpaw Creek as noted above. Within this context, we map a south-dipping thrust fault along the topographic lineament, with a splay fault offsetting the Nanushuk beds near Bearpaw Creek (sheet 1 and fig. 7).

We also reconnoitered a normal fault near Umiat Mountain (Houseknecht and Schenk, 2005; fig. 7 and sheet 1; compare to Brosgé and

Whittington, 1966) that lies approximately 1 km southeast of the eastern end of the lineament (fig. 7). This fault dips approximately 45° toward approximately 125°, has a m-scale shear zone with locally boudinaged sandstone, and is associated with numerous smaller-scale normal-slip faults that dip moderately to steeply east/east-southeast and west/west-northwest, accommodate tens of centimeters of dip slip, and locally host secondary shear steps on non-mineralized, polished, striated slip planes. Houseknecht and Schenk (2005) inferred approximately 120 m of stratigraphic separation across the main fault plane, which juxtaposes Seabee (footwall) and Tuluvak (hanging wall) Formations in the upper part of the exposure (fig. 7). Fault orientations in this area in part coincide with the east-dipping normal fault in the 11BG269/11BG270 area.

In addition to the field relations outlined above, well and seismic data provide constraints on the nature of faulting associated with the Umiat anticline. The recognition of repeated stratigraphic intervals in Umiat oil field wells indicate thrust faults at depth (Collins, 1958; Brosgé and Whittington, 1966; Molenaar, 1982; this study). Variability exists among the published seismic interpretations, some of which is undoubtedly related to varying degrees of data quality (see Brosgé and Whittington, 1966; Molenaar, 1982; Kumar and others, 2002; Hanks and others, 2014; Sanders, 2014; this study). Kumar and others (2002) did not pick faults above the lower Brookian (their Fortress Mountain Formation; broadly equivalent to the lower part of our Torok Formation), and Sanders (2014) depicted only one fault cutting the Nanushuk (a subordinate, north-dipping thrust in the anticline's south limb). However, most of the publicly available seismic interpretations include south-dipping thrust faults that ramp up from mid-Torok, cut into the Nanushuk and overlying stratigraphy, and project toward the topographic lineament in the north limb of the anticline. Such interpretations are consistent with our work (sheet 1: cross section A–A'). Structure mapping by Hanks and others (2014) of three-dimensional seismic data yielded a fault pattern similar to the mapped fault pattern of sheet 1.

Discussion and Summary of Umiat Oil Field Structure

Geologic mapping of the Umiat anticline's north limb documents a pattern of increasingly younger stratigraphic units to the north. Although this trend in the distribution of map units is predicted in association with a gentle fold in a region of low-relief topography, the uncharacteristically steep bedding dips and truncated or absent stratigraphic units near the lineament support the interpretation that one or more faults cut(s) the north limb of the Umiat anticline in this area. In detail, there is some variability in how the stratigraphy has been mapped near the lineament. Brosgé and Whittington (1966; see also Molenaar, 1982), employing a different stratigraphic nomenclature than later studies, mapped multiple Seabee units in their fault zone, with lowermost Tuluvak (their Ayiyak Member of the Seabee Formation) locally mapped south of the northern margin of the zone; overlying Tuluvak strata (their Tuluvak Tongue of the Prince Creek Formation) are mapped directly north of the fault zone along most of its extent, and Nanushuk lies to the south at Bearpaw Creek and in a small area to the west (compare with sheet 1). Alternatively, Mull and others (2004) and this study approximately map the southern margin of the Brosgé and Whittington (1966) fault zone as a single fault trace with Nanushuk, and in large part Seabee, lying south of the fault and Tuluvak mainly to the north.[7] Nevertheless, stratigraphic relations across the fault zone of Brosgé and Whittington (1966) are consistent with stratigraphic relations across the single fault trace mapped by Mull and others (2004) and on sheet 1.

The Nanushuk–Tuluvak juxtaposition—with the approximately 400-m-thick Seabee (see below) being locally absent—across the fault/fault zone at Bearpaw Creek (sheet 1) establishes the minimum stratigraphic separation at this locality. Stratigraphic observations of this study and those reported by previous workers seemingly require any fault or fault zone mapped along the lineament to be a south-dip-

[7]This discussion focuses on the main fault of sheet 1/figure 7 and does not explicitly address the smaller-scale and limited extent splay fault that offsets Nanushuk beds by several tens of meters near Bearpaw Creek.

ping thrust fault or a north-dipping normal fault; setting aside complex, multi-phase deformation scenarios such as an inverted normal fault with less post-inversion dip slip, neither of these scenarios is readily compatible with the north-dipping thrust interpretation of Mull and others (2004). In addition to the surface relations noted, numerous studies of various vintages of seismic data and well logs, including our work, concluded that a south-dipping thrust fault/zone ramps up from the Torok south of the axial surface and cuts into the post-Torok stratigraphy in the north limb of the Umiat anticline, projecting toward or breaching near the lineament of figure 7. Ultimately, we do not find this interpretation to be equivocal or controversial, but rather that the available surface and subsurface evidence strongly supports the interpretation of a south-dipping thrust associated with the Umiat oil field as conveyed in cross section A–A' (sheet 1).

The minor normal faults in the vicinity of 11BG269/11BG270 and the larger normal fault at Umiat Mountain at least in part post-date lithification, as evidenced by mineralized, polished, and stepped shear planes. These faults are thus probably not related to the basinward dipping normal faults and slumps of Houseknecht and Schenk (2005; fig. 3 therein), which are mapped in seismic data and reflect Cretaceous basin-fill architecture and soft-sediment deformation processes (see also Decker, 2007). In fact, the normal faults that we examined may simply represent strain partitioning related to the locally doubly plunging Umiat anticline near Umiat and the larger-scale trend of diminishing structural relief to the east-southeast beyond the Colville River (fig. 5). The faults at 11BG269 and 11BG270 may in part record bedding parallel flexural slip during folding of mechanically rigid successions of Tuluvak. In other words, the normal-slip faults of this study may be associated with Paleocene fold-and-thrust belt contraction; additional considerations of along-strike distribution of strain are included below.

Colville River Corridor Structure

The Colville River in the Umiat region occupies an approximately 3–5-km-wide floodplain that maintains a broadly linear, northeastward trend for more than 100 km from Killik Bend to Shivugak Bluff (fig. 1). This trend, the northeastern part of which lies in the map area, extends obliquely across the structural grain of the foothills fold-and-thrust belt. Quaternary deposits of the floodplain obscure structural relations across the Colville River, and locally excellent bluff exposures rarely occur where there are good outcrops on the opposite bank. Despite somewhat limited outcrop control for detailed correlations of structures across the river, there are indications that structural changes occur at or adjacent to this reach of the Colville River (Brosgé and Whittington, 1966; Mull and others 2004, 2005; this study; see also Detterman and others, 1963). As an example, in the Umiat–Gubik map area, Mull and others (2004) noted that the Fossil Creek anticline becomes more structurally complex approaching the Colville River from the east, and they do not map this anticline northwest of the river (compare to sheet 1). Mull and others (2004) also highlighted the structural complexity of the Umiat anticline at the Umiat oil field and the change to an east-trending axial trace near the Colville River despite the fold's regional southeast trend. These field relations, among others, led Mull and others (2004, 2005) to map a regional-scale, left-lateral strike-slip fault—their Colville fault—along the Colville River floodplain from Killik Bend to beyond Shivugak Bluff (see also footnote 4). Two Colville fault segments were mapped within our study area, with an overlapping left step near the mouth of Prince Creek (Mull and others, 2004). The Colville fault was described as a deep-seated wrench fault having no more than a few miles of offset, post-dating and cutting across the early Cenozoic foothills fold-and-thrust belt, and accounting for local structural complexities, deflected axial traces, fold axis terminations, and apparent en-echelon fold patterns.

A Colville River fault has implications for the style of deformation and trap geometries in the foothills petroleum province of the North Slope, but the existence of such a fault remains equivocal. Presented below are new fracture plane data

collected during this study to address the Colville fault hypothesis.

Fracture Study–Evidence for a Colville Fault?

The Colville fault is not mapped in outcrop, but many of the Colville River bluff exposures lie within tens of meters to several kilometers of the interpreted trace (Mull and others, 2004, 2005). We measured fracture planes and kinematic indicators, where present, in Colville River corridor outcrops at the Colville incision and Fossil Creek bluff localities as well as at Tattitgak Bluff, Umiat Mountain, and Shivugak Bluff (fig. 1; appendix 2). Our goal in collecting these data was to determine whether outcrop-scale brittle structures in these areas reflect a larger-scale, left-lateral strike-slip fault with a principal displacement zone (PDZ; that is to say, the Colville fault of Mull and others [2004]) lying under the Colville River's broad floodplain.

Premise

Laboratory models of strike-slip faults deformed in simple shear indicate that subordinate structures form in predictable orientations with respect to a PDZ that accumulates slip parallel to the applied shear direction (see reviews by Christie-Blick and Biddle, 1985; Sylvester, 1988). Figure 8 summarizes orientation and sense of slip relations among structures that may develop in such a strike-slip fault system: 1) strike-slip shear fractures, including Y (synthetic; parallel to PDZ), R and P (synthetic), and R' (antithetic; conjugate to R); 2) T or extension fractures (mode 1 cracks) and normal faults that strike perpendicular to the minimum principal stress; and 3) thrust faults and folds that strike perpendicular to the maximum principal stress. These idealized structures and their orientations are not universally observed in association with strike-slip deformation, with complications arising from the typical heterogeneity of rocks and the commonly protracted, rotational, and cross-cutting nature of strike-slip fault systems (Christie-Blick and Biddle, 1985; Sylvester, 1988). Nevertheless, documenting the presence or absence of subordinate structures is one approach toward better understanding larger-scale strike-slip faults that may not be directly expressed in outcrop.

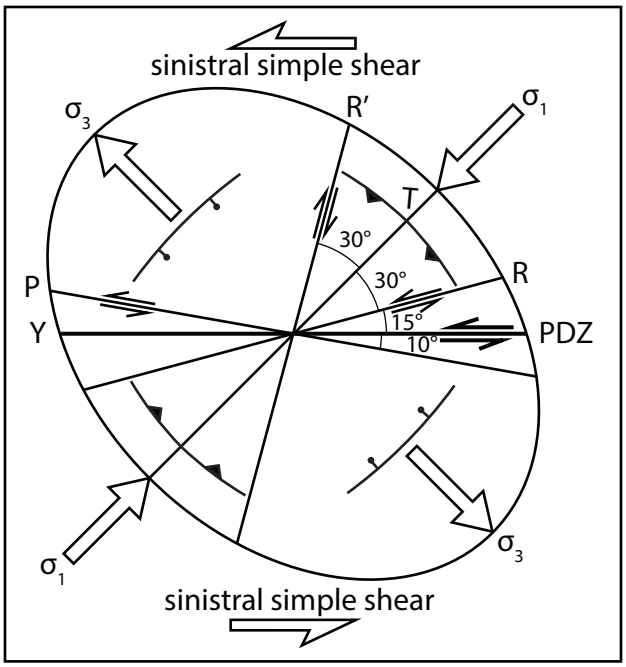

Figure 8. Idealized strain ellipse for left-lateral strike-slip fault system in simple shear. Structures that might form in the noted stress and strain fields are designated. Principal stress axes are oriented 45° from the principal displacement zone (PDZ). Sigma-1 is the maximum principal stress direction; sigma-3 is the minimum principal stress direction; principle stress arrows depicted here are not quantitative vectors. Figure modified from Christie-Blick and Biddle (1985), Sylvester (1988), and Twiss and Moores (1992); see also McClay (1987).

Data, Results, and Strain Ellipse Comparisons

We measured 493 fractures, sampling an approximately 45-km-long segment of the Colville River's northeast-trending reach (fig. 9). Most of the fractures (n=453 of 493; 91.9%) lack shear indicators; the remaining fractures (n=40 of 493; 8.1%) have evidence of shear, but only 23 of these are uniquely constrained kinematically (fig. 10; appendix 2). The Colville incision and Fossil Creek bluff localities each have two fracture sets with relatively low scatter; the Tattitgak and Shivugak Bluffs and Umiat Mountain localities each host numerous fracture sets (n>2) with relatively high scatter and common outliers (fig. 9). There is a clear geographic component to variability in the Colville River bluff fractures data—

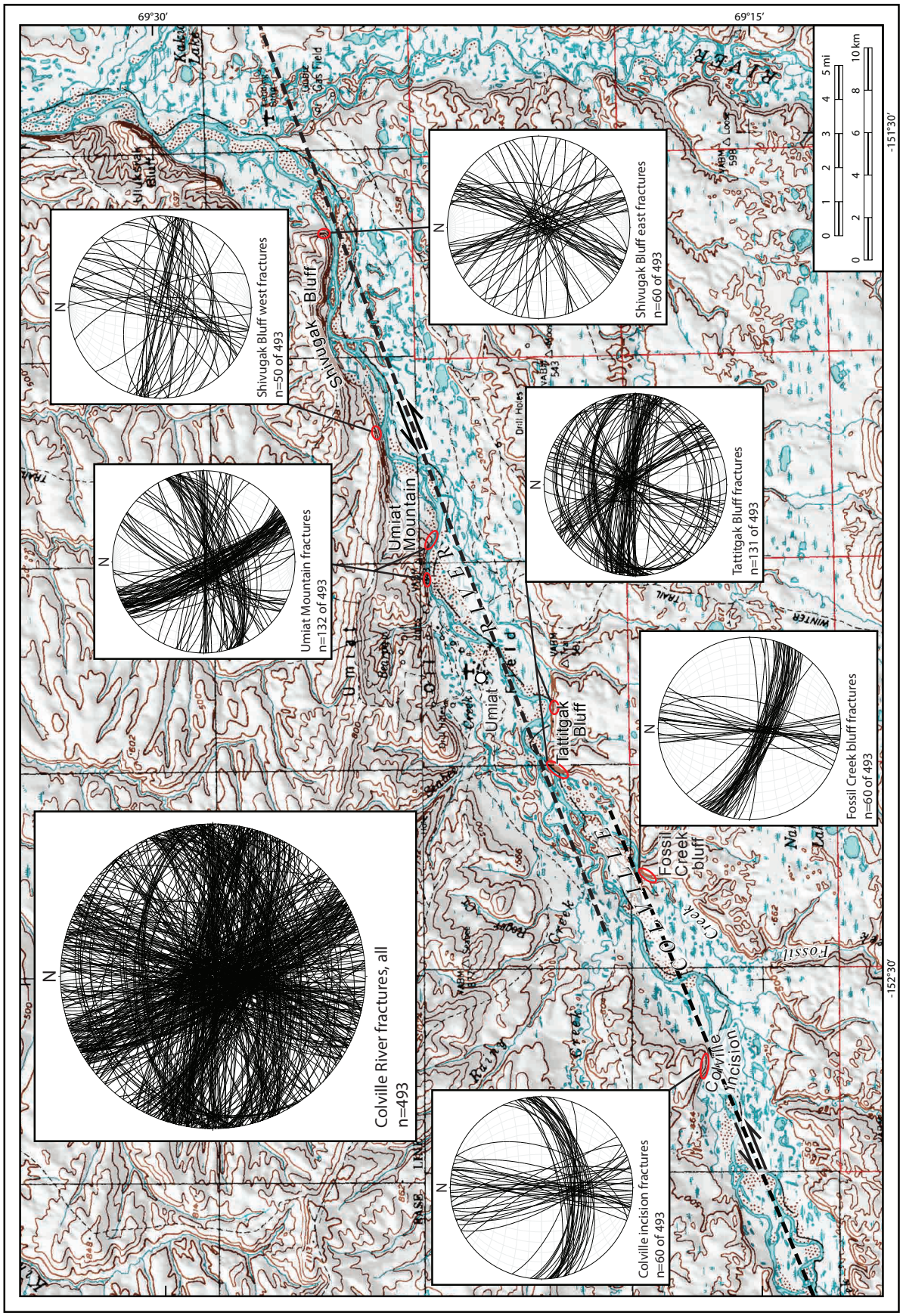

Figure 9. Equal area stereonet plots of all Colville River fracture data (n=493; upper left of figure) and plots of fractures measured at each collection area. Note thick, short-dashed line delineating the trace of the hypothesized left-lateral Colville fault as mapped by Mull and others (2004). Fracture data plotted in Stereonet 9.8.3 (©Richard W. Allmendinger; see Allmendinger and others, 2013; Cardozo and Allmendinger, 2013). See figure 1 for location context. Topographic base map from part of U.S. Geological Survey Umiat 1:250,000-scale quadrangle map.

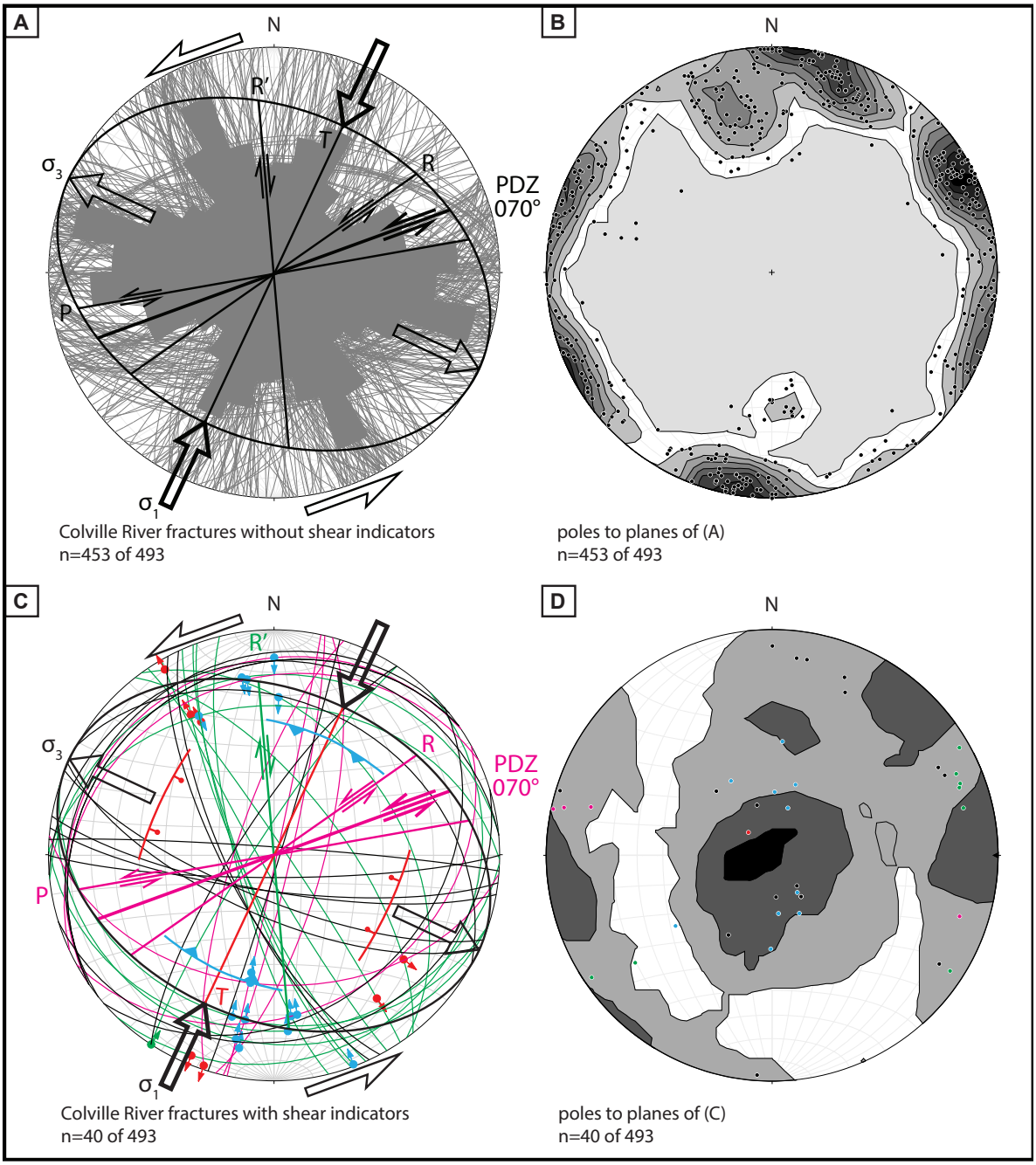

Figure 10. A. Equal area stereonet plot of Colville River fractures that lack indications of shear. Rose diagram strike-orientation petals are bi-directional and scaled to length. See text for discussion of fracture data with respect to the idealized simple shear strain ellipse. **B**. Poles to planes of A. **C**. Equal area stereonet plot of Colville River fractures that have indications of shear. Great circles are color-coded to strike component of slip: magenta indicates left lateral and green indicates right lateral. Striae (points along great circles) with hanging wall slip direction (arrows originating on striae) are color-coded to dip component of slip: blue indicates reverse and red indicates normal. Note that one fault has no dip-slip component and the stria and arrow are both color-coded to the strike component of slip. Shear fractures that lack unique kinematic constraints are plotted as black great circles without striae. See text for discussion of fracture data with respect to the idealized strain ellipse. **D**. Poles to planes of C. Poles are color-coded with principal component of slip as in C. Kamb contours of B and D plotted at intervals of two standard deviations. Fracture data of A, B, and D plotted in Stereonet 9.8.3 (see references above); shear fracture data of C plotted in FaultKin 7.4.3 (©Richard W. Allmendinger; see Marrett and Allmendinger [1990] and Allmendinger and others [2013]). See figure 8 and Premise section above for abbreviation explanation and stress arrow descriptions. A spreadsheet of fracture data is presented in appendix 2.

and there are no wholly repeated fracture set patterns among the stereonet plots of figure 9—although there are several fracture sets that occur at more than one locality. In the following evaluation of the fracture data with respect to a simple shear strain ellipse (fig. 8), we employ a PDZ that strikes 070° (fig. 10), paralleling the northeastern Colville fault segment of Mull and others (2004).

The non-shear fracture dataset (figs. 10A and B) dominantly comprises steeply dipping planes, with the majority of these surfaces dipping greater than 80°; only 10.6 % (n=48 of 453) of these fractures dip less than 60° and none dip less than 40° (see fig. 10B). Binning these data in 10° strike-orientation intervals outlines several prominent fracture orientations, although there are fractures that lie in every one of these bi-directional rose diagram petals. Comparing the visually prominent petals of figure 10A with the idealized strain ellipse suggests some possible matches for structures subordinate to the potential PDZ. The strongest correlation is a candidate match for T fractures in the 020–030° rose petal bin (fig. 10A). T fractures, which are mode 1 cracks, would, by definition, be expected to occur as joints (see Biddle and Christie-Blick, 1985), which is consistent with the non-sheared nature of these fractures. Additional correlations are less clear. There are, at a minimum, candidate fractures for Y (parallel to PDZ) and P shears, but there is a wide spread of the data in this segment of the stereonet (that is to say, 060–090°; fig. 10A) and lack of shear evidence on these fracture planes. Two of the most prominent non-sheared fracture orientations are south-southeast and east-southeast-striking and do not coincide with any predicted orientations of subordinate structures in the idealized strain ellipse (fig. 10A). None of the dominant petals are coincident with the predicted orientations of either synthetic or antithetic Riedel shears (that is to say, R or R').

The shear fracture dataset (figs. 10C and D) comprises a bi-modal distribution of dip magnitudes, with 55.0% (n=22 of 40) of the planes dipping 66–89° and the remainder dipping less than 45° (see fig. 10D). There is a wide spread of strike orientations among these data, which include 23 planes with unique kinematic constraints: reverse-left-slip (n=7); normal-left-slip (n=1); reverse-right-slip (n=8); normal-right-slip (n=6); and right-lateral strike-slip (n=1). Comparison of the shear fracture data with the idealized strain ellipse indicates potential correlations (fig. 10C). Three shear fractures strike within 10° of the predicted maximum principle stress direction (025°) and are consistent with the predicted normal fault orientation (fig. 10C). These three fractures—two of which are not uniquely kinematically constrained and the third being a left-lateral strike-slip fault with only a minor component of normal slip—dip steeply (77–88°). Three additional planes with similar strikes also dip steeply but are dominantly strike-slip faults with minor components of reverse slip. There are five shear fractures that strike within 10° of the predicted minimum principle stress direction (115°) and are thus consistent with the predicted thrust fault orientation (fig. 10C). Two of these fractures dip gently (18° and 27°) and are dominantly reverse-slip faults, and a third shear fracture lacks unique kinematic constraints but dips a moderate 34°; the remaining two planes also lack unique kinematic constraints and are less ideal candidates for thrust faults due to their steep dips (68° and 74°). Steeply dipping shear fractures that lie within 10° of strike of the idealized strike-slip faults include one R' candidate (dominantly strike-slip; minor reverse component of slip) and one P candidate (not uniquely kinematically constrained); PDZ/Y and R candidates are absent from the shear fracture dataset (fig. 10C).

Additional Considerations and an Alternative Hypothesis for the Fracture Data

The fracture data presented above and compared to the simple shear strain ellipse of figure 10 include candidate structures that may reflect a regional-scale, left-lateral strike-slip fault striking 070°. However, there are few of these candidate planes, and the most prominent fracture sets, with the exception of possible T fractures, are not accounted for by the simple shear model (fig. 10). This dataset also has relatively few planes with

shear indicators (n=40 of 493), and there is evident geographic variability to the fracture orientations, which is consistent with work by Hanks and others (2014). Ultimately, there is a dearth of evidence from the fracture data to infer a large, left-lateral strike-slip fault along the Colville River.

Additional observations and data also bear on an evaluation of the Colville fault hypothesis. Our seismic-based mapping of fold axial traces near the Colville River do not readily permit mapping a through-going, left-lateral strike-slip fault with many miles or kilometers of offset (compare figs. 11A and B). Although some fold axis trends are seemingly consistent with progressive accumulation of slip along a left-lateral strike-slip fault system at the Colville River, there are problematic aspects to such an interpretation. As an example, the idealized fold axes in the strain ellipses of figure 11 are modeled after progressive deformation of en echelon folds that form and deflect *during* accumulation of strain in the PDZ. In other words, en echelon fold axes that are genetically tied to strike-slip deformation undergo progressive rotation toward parallelism with the master fault as slip continues to accrue and strike-slip related folding propagates farther from the PDZ (Harding and Lowell, 1979; Sylvester, 1988). No work to date has suggested that the folds in the study area developed in a regional strike-slip regime, so any apparent similarities between deflected, en echelon fold axes associated with strike-slip fault systems may be coincidental.

The fold map pattern of this study (sheet 1 and fig. 11B) may simply reflect fold-and-thrust belt evolution. For example, in our examination of seismic data along the Umiat anticline near the Colville River, disruption of seismic character along an apparently sub-vertical plane and apparent offset of the fold axis suggest right-lateral strike-slip separation across the axial surface at the Colville River (see tear fault(?) of sheet 1). This structure is potentially a tear fault that accrued right-lateral strike-slip offset during detachment folding and associated thrust faulting, with the western part of the fold propagating farther basinward and having greater structural relief than the same structural culmination to the east (fig. 5 and sheet 1). We do not map the candidate tear fault as extending for more than 5 km along the Colville River floodplain, although seismic constraints are less robust beyond the fold's axis. This structure may have also partly accommodated the notable change in along-strike structural character of the Umiat anticline across the Colville River, with a north-dipping breaching back-thrust interpreted in seismic data near the East Umiat gas field versus the south-dipping thrust at the Umiat oil field (compare cross sections A–A' and B–B' of sheet 1). Therefore, deflection of fold axes in the study area may be tied to the distribution of shortening both along strike and across the mechanical stratigraphy, which may locally render tear faults that cut across the regional structural grain but do not extend continuously across the fold-and-thrust belt for tens or hundreds of kilometers. Further along-strike strain partitioning related to varying degrees of structural relief may also be accommodated by the normal faults reported and discussed above.

An alternative interpretation of this study's fracture dataset is presented in figure 12, which highlights potential correlations of the measured fractures with respect to a Coulomb-Anderson pure shear model of deformation (for example, see Sylvester, 1988) for the Brooks Range foothills fold-and-thrust belt. The non-shear fracture dataset contains hundreds of steeply dipping planes that strike within approximately 15° of a hypothetical set of conjugate strike-slip fractures oriented 30° from a reasonably permissible north–south maximum principle stress direction (figs. 12A and B). Abundant, steeply dipping, east-northeast- to east-southeast-striking, non-shear fractures may be associated with folding (see axial planar joints(?) of fig. 12B), and some of the geographic variability of fracture orientations noted above and evident in figure 9 may also reflect fold-related fractures (compare with Twiss and Moores, 1992, p. 48–50). Furthermore, the shear fracture dataset includes dozens of planes with orientations—and in many cases unique slip indicators—

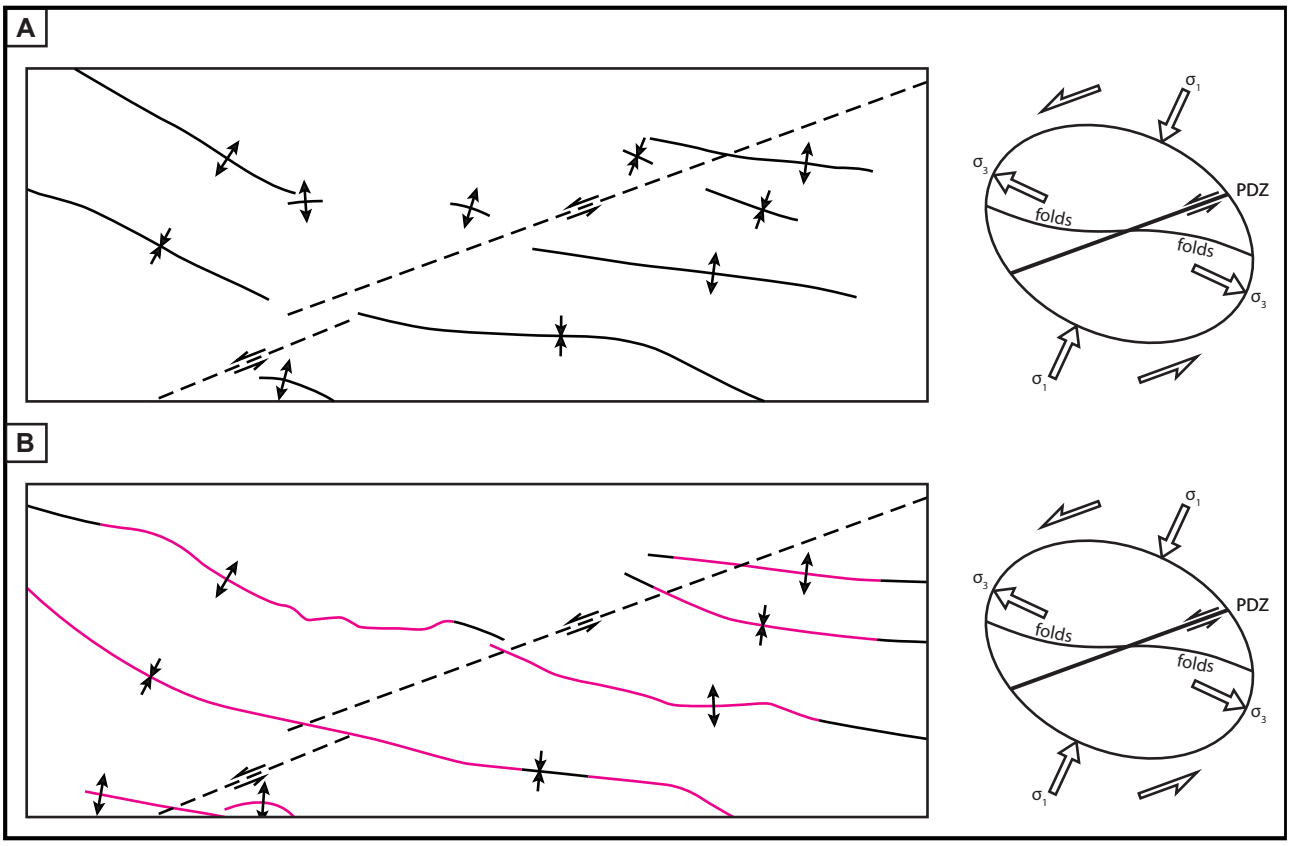

Figure 11. Axial trace line drawings for folds in the Umiat–Gubik map area from Mull and others (2004) (**A**) and this study (**B**). Left-lateral strike-slip faults in A and B are the Colville fault of Mull and others (2004), but note that we do not map this fault on sheet 1; see text for discussion. See sheet 1 for map symbol explanation. Strain ellipses at right are modified from Sylvester (1988); see also figure 8 for strain ellipse symbol and abbreviation explanation.

that are consistent with predicted conjugate strike-slip faults and thrust faults (figs. 12C and D). In other words, the n=493 fracture dataset collected to test the Colville fault hypothesis may chiefly reflect strain associated with north–south contraction during the main phase of Paleogene orogenic deformation described above.

Strike-slip faults are commonly difficult to characterize, and the fracture analysis presented here does not rule out the permissibility of regional strike-slip faulting as described by Mull and others (2004, 2005). However, we do not map the Colville fault on sheet 1 due to the lack of compelling surface or subsurface evidence for a through-going, left-lateral strike-slip fault along the Colville River. Furthermore, our fracture-scale to map-scale structural observations are more readily accounted for within the context of pure shear, contractional fold-and-thrust belt deformation. Nevertheless, future studies in the central Brooks Range foothills fold-and-thrust belt will undoubtedly further constrain the style and timing deformation, the distribution of shortening, and the nature of smaller-scale faulting, all of which have implications for further understanding petroleum systems in this gas-prone region of northern Alaska.

DESCRIPTION AND INTERPRETATION OF MAP UNITS

Surficial Deposits

Quaternary deposits described below are modified from the 1:250,000-scale surficial geologic map of the Umiat Quadrangle (Carter and Galloway, 1986). See also Stevens and others (2003) for derivative geologic mapping along potential access corridors in the Umiat area (see also Reger and others, 2003).

Qal ALLUVIAL DEPOSITS (Quaternary)—Undifferentiated alluvium,

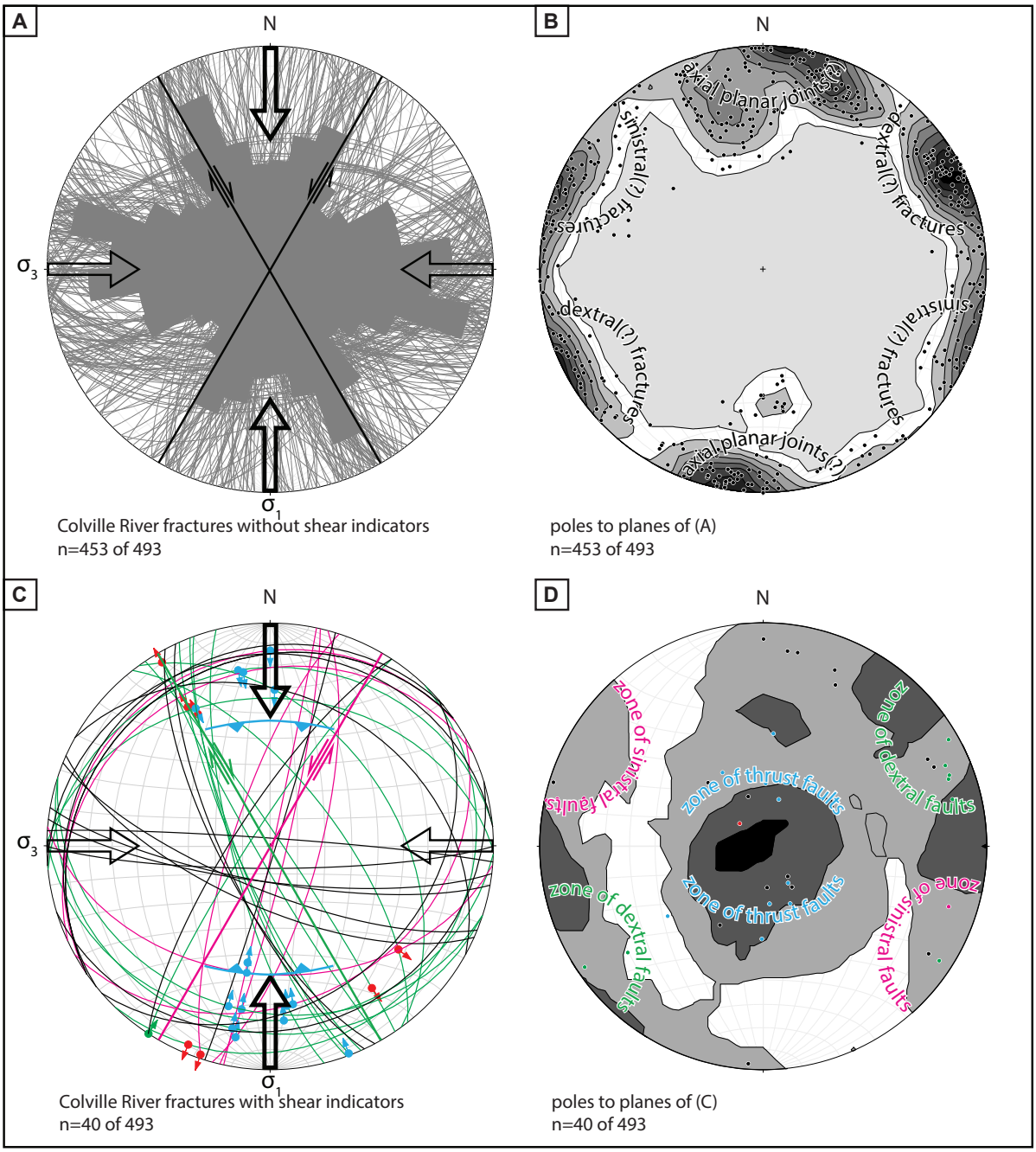

Figure 12. Stereonet plots of fracture data are the same as presented in figure 10, but here are interpreted within the context of the east-trending central Brooks Range foothills fold-and-thrust belt and a pure shear deformation model. See text for discussion of fracture data with respect to north–south shortening. **A**. Equal area stereonet plot of Colville River fractures that lack indications of shear. Conjugate strike-slip faults are plotted at 30° from sigma-1, which is oriented north–south. Rose diagram strike-orientation petals are bi-directional and scaled to length. **B**. Poles to planes of A. **C**. Equal area stereonet plot of Colville River fractures that have indications of shear. Great circles are color-coded to strike component of slip: magenta indicates left lateral and green indicates right lateral. Striae (points along great circles) with hanging wall slip direction (arrows originating on striae) are color-coded to dip component of slip: blue indicates reverse and red indicates normal. Note that one fault has no dip-slip component and the stria and arrow are both color-coded to the strike component of slip. Shear fractures that lack unique kinematic constraints are plotted as black great circles without striae. **D**. Poles to planes of C. Poles are color-coded with principal component of slip as in C. Kamb contours of B and D plotted at intervals of two standard deviations. Fracture data of A, B, and D plotted in Stereonet 9.8.3 (see references above); shear fracture data of C plotted in FaultKin 7.4.3 (see references above). Sigma-1 is the maximum principal stress direction; sigma-3 is the minimum principal stress direction; principle stress arrows depicted here are not quantitative vectors.

including deposits of active and abandoned fluvial channels, as well as floodplains and alluvial terraces up to 8 m above modern streams. Chiefly comprises stratified deposits of fine- to coarse-grained sand, silty to gravelly sand, and gravel. Modified from Carter and Galloway (1986).

Brookian Megasequence

The Brookian megasequence (Lerand, 1973; Molenaar, 1983; Hubbard and others, 1987) is the stratigraphic record of Brooks Range orogenesis, with incipient Colville foreland basin sedimentation commencing as early as the Jurassic (Bird and Molenaar, 1992). The foreland basin of what is now the central North Slope was filled during the mid- to Late Cretaceous by a chiefly northeastward prograding siliciclastic wedge, with detritus sourced from the Brooks Range at the basin's southern margin and farther west in the area of the modern Chukchi Sea (Bird and Molenaar, 1992). Portions of three major Brookian depositional cycles occur in the Umiat–Gubik map area: 1) Nanushuk–Torok (Ahlbrandt, 1979; Huffman, 1985; Huffman and others, 1988; Molenaar, 1985, 1988; Houseknecht and Schenk, 2001; Houseknecht and others, 2009; LePain and others, 2009); 2) Tuluvak–Seabee (Mull and others, 2003; Houseknecht and Schenk, 2005; Decker, 2007); and 3) Prince Creek–Schrader Bluff–Canning (Molenaar and others, 1987; Mull and others, 2003; Decker, 2007) (fig. 4). All of these formations except the Torok and Canning are recognized in outcrop in the study area (Detterman and others, 1963; Brosgé and Whittington, 1966; Mull and others, 2003, 2004; this study). Deep-water Torok underlies the area and influenced the depositional architecture of overlying units (see below) and the structural evolution of the fold-and-thrust belt (see above). However, deep-water Canning Formation does not occur in the Umiat–Gubik area subsurface, as it was deposited beyond the earliest Schrader Bluff Formation shelf edge established east of the Anaktuvuk River (see below).

The exposed stratigraphy dominantly records shallow-marine, basin-scale topset sedimentation. Houseknecht and Schenk (2005) also reported that prodelta, seismic-scale Seabee Formation clinoforms prograded across the draped, inherited depositional profile of the Nanushuk shelf; this Seabee clinoform seismic facies is inferred to crop out at Umiat Mountain. Regional stratigraphic work indicates that the topset units of the Umiat area grade basinward into correlative foreset (slope) and bottomset (basin floor) facies (for example, Huffman, 1985; Molenaar, 1988; and Decker, 2007); all of these lithostratigraphic units ultimately condense eastward into the distal Hue Shale (fig. 4). Recent detailed geologic mapping in the Sagavanirktok River (Gillis and others, 2014) and Gilead Creek (Herriott and others, in preparation) areas (fig. 1) further document the proximal–distal stratigraphic relations that developed and evolved through time and space during mid-Cretaceous to Paleogene filling of the Colville foreland basin in the central to east-central North Slope.

Stratigraphic Nomenclature

The stratigraphic nomenclature of the Colville foreland basin fill succession has undergone major revisions since the pioneering work by Schrader (1902, 1904) and Leffingwell (1919). The Pet-4 program (see above) yielded numerous insights into the stratigraphic framework of the basin (Gryc and others, 1951; Gryc, 1956), rendering a more detailed understanding of the stratigraphy than had previously been established. Subsequent stratigraphic revisions for the region were summarized by Kopf (1970) and Bird (1988b). More recent work by Mull and others (2003), building on decades of detailed stratigraphic studies, presented a markedly revised stratigraphic nomenclature for Cretaceous and Cenozoic units of the central and western Colville basin. This simplified framework aimed to clarify the geologic context of the basin's deposits and to provide more consistently mappable units with regional significance. The current study employs the stratigraphy of Mull and others (2003), with the noted exception that we continue to recognize and map in the Umiat–Gubik area the Schrader Bluff Formation Members—Sentinel Hill, Barrow Trail, and Rogers Creek—in the sense of Detterman and others (1963) and Brosgé and Whittington (1966)

(see below for further discussion); we retained these members due to their mappability and utility in defining structural map patterns and stratigraphic evolution.

A significant body of literature addressing the geology of the Umiat region predates the stratigraphic revisions by Mull and others (2003). Basic stratigraphic equivalencies relevant to the study area and with respect to the work of Mull and others (2003) include: 1) all former tongues and formations of the Nanushuk Group (abandoned/demoted) are the Nanushuk Formation; 2) the former Colville Group (abandoned) is the non-grouped Seabee, Tuluvak, Schrader Bluff, and Prince Creek Formations; 3) the former Shale Wall Member (abandoned) of the Seabee Formation is the Seabee Formation; 4) the former Ayiyak Member (abandoned) of the Seabee Formation is the lower, marine part of the Tuluvak Formation; 5) the former Tuluvak Tongue (abandoned) of the Prince Creek Formation is the upper, nonmarine part of the Tuluvak Formation; 6) the former Rogers Creek, Barrow Trail, and Sentinel Hill Members (abandoned) of the Schrader Bluff Formation are the undivided Schrader Bluff Formation (see above and below regarding our continued usage of these members); and 7) the former Kogosukruk Tongue (abandoned) of the Prince Creek Formation is the Prince Creek Formation.

PRINCE CREEK FORMATION (regionally Campanian–Paleocene: see review by Mull and others, 2003) (defined and/or locally mapped by Gryc and others, 1951; Whittington, 1956; Detterman and others, 1963; Brosgé and Whittington, 1966; revised by Mull and others, 2003, 2004)—The Prince Creek Formation (fig. 13) comprises nonmarine deposits in chiefly prograding and aggrading depositional systems that were associated with shallow-marine equivalents of the Schrader Bluff Formation (Molenaar, 1983; Mull and others, 2003; Decker, 2007; Flores and others, 2007a, 2007b; van der Kolk and others, 2015) (fig. 4). Van der Kolk and others (2015) generally interpreted the Prince Creek Formation at Shivugak Bluff as comprising distributary and braided fluvial deposits that are progradationally stacked on deltaic strata of the Sentinel Hill Member (Schrader Bluff Formation). Only the older (Upper Cretaceous) part of the Prince Creek crops out in the map area (fig. 4); the best exposures of the unit are mapped at Shivugak and Uluksrak Bluffs (figs. 3B and 13) and along the west bank of the Anaktuvuk River (sheet 1).

The revised Prince Creek Formation (Mull and others, 2003) in the Umiat region is a minimum 552 m thick as reported by Brosgé and Whittington (1966), who recognized a 96-m-thick tongue of marine rocks along the Uluksrak Bluff trend that they regarded, but did not map, as an upper part of the Sentinel Hill Member. However, documented stratigraphic relations indicate that any intra-Prince Creek marine deposits of the Shivugak and southern Uluksrak Bluffs area would probably lie above the regionally significant mid-Campanian unconformity (MCU) of Decker (2007) (Flores and others, 2007a; van der Kolk and others, 2015). Therefore, any marine succession encased in nonmarine Prince Creek in the Umiat–Gubik area likely correlates to the regional middle Schrader Bluff Formation (in the sense of Decker, 2007) and should not be regarded as an upper part of the Sentinel Hill Member, which is distinctly part of the regional lower Schrader Bluff Formation (see fig. 4 and discussion below). Farther north at the Sentinel Hill Core No. 1 well (~20 km north-northeast of Shivugak Bluff) the MCU's location with respect to thick intercalations of nonmarine (Prince Creek) and marine (Schrader Bluff) successions was documented by Flores and others (2007b). Nevertheless, any marine intervals hosted in the Prince Creek Formation of the Colville River area likely record smaller-scale retrogradation during transgressions in the dominantly progradational/aggradational Prince Creek–Schrader Bluff couplet (Mull and others, 2003; Decker, 2007; Flores and others, 2007a, 2007b).

TKpc PRINCE CREEK FORMATION (locally late Campanian–middle-late Maastrichtian: Flores and others, 2007a)—Light- to dark-brown- to gray-brown-

Figure 13. Field photographs of Prince Creek Formation. **A**. Oblique aerial view northeastward of a thick Prince Creek Formation succession at southwestern end of Uluksrak Bluff. Contact with the underlying Sentinel Hill Member (Schrader Bluff Formation; see red arrow) is consistent with our mapping of Shivugak Bluff. Note repeating stratigraphic motif of thick, erosionally resistant, fluvial sandstone successions, which are locally conglomeratic, that are separated by thicker, less resistant, finer grained, and thinner bedded intervals. The lateral discontinuity of some of the resistant sandstone packages is evident in this km-scale outcrop extent. Topographic relief of bluff at right of photograph is ~90 m, for sense of scale. **B**. Outcrop-scale view of fluvial sandstone succession in Prince Creek comparable to resistant packages of A. This ~6-m-thick cliff-forming section crops out near the top of Shivugak Bluff. Black backpack is ~60 cm tall. **C**. Detailed view of cross-stratified sandstone and pebbly sandstone of Prince Creek. This outcrop lies in the north limb of the Gubik anticline between Shivugak and Uluksrak Bluffs. Hammer is 31 cm long. Photographs by T.M. Herriott.

weathering, dominantly light-gray, thick- to very thick-bedded, moderately indurated, commonly cross-stratified (foreset amplitudes to greater than 1 m), quartzose pebbly sandstone, fine- to coarse-grained sandstone, and conglomeratic lag deposits, with subordinate gray to dark-gray, chiefly thin- to medium-bedded, carbonaceous

to bentonitic very fine-grained sandstone and mudstone, as well as medium- to very thick- bedded, dull to bright-and-dull-banded lignitic to subbituminous coal. The cross-stratified sandstone and pebbly sandstone lithofacies have scoured, sharp basal contacts and cm-scale, coalified woody debris is commonly observed; pebbles (commonly 1.5 cm long-axis dimension) are subangular to subrounded and generally comprise vein quartz and cherty argillite; both the pebble and sand fractions exhibit salt-and-pepper-like compositional coloring. Very fine-grained sandstone and mudstone facies are commonly rusty-orange- to tannish-yellow-weathering, and root traces are locally observed.

SCHRADER BLUFF FORMATION (regionally Santonian–Maastrichtian: see review by Mull and others, 2003; as young as Paleocene(?): see Decker, 2007) (defined and/or locally mapped by Gryc and others, 1951; Whittington, 1956; Detterman and others, 1963; Brosgé and Whittington, 1966; revised by Mull and others, 2003, 2004)—The Schrader Bluff Formation comprises the record of shallow-marine depositional systems that interfingered with nonmarine Prince Creek Formation along transgressive–regressive paleoshorelines, principally rendering progradational and aggradational topsets of this basin-scale depositional cycle (Molenaar, 1983; Mull and others, 2003; Decker, 2007; Flores and others, 2007a, 2007b; van der Kolk and others, 2015) (fig. 4). The base of the Schrader Buff Formation transgressively overlies the Tuluvak Formation. Van der Kolk and others (2015) described the upper part of the Schrader Bluff Formation (Sentinel Hill Member) at Shivugak Bluff as comprising muddy, river-dominated deltaic strata. Following Detterman and others (1963), Brosgé and Whittington (1966), and the criteria described by Mull and others (2003), we map the upper contact of the Schrader Bluff at the onset of nonmarine sedimentation of Prince Creek.

Early detailed studies of the Schrader Bluff Formation were by Gryc and others (1951), with subsequent work in the Umiat region leading to the definition of three members, in descending order: Sentinel Hill (fig. 14), Barrow Trail (fig. 15), and Rogers Creek (fig. 16) (Whittington, 1956; Detterman, 1956a; Detterman and others, 1963; Brosgé and Whittington, 1966). However, in a regional context, these members—including the formation's type section along the east bank of the Anaktuvuk River at Schrader Bluff (fig. 1)—constitute only the lower of three regional parts in the formation (fig. 4). This lower part of the Schrader Bluff comprises mid-Campanian and older (Santonian) strata that occur entirely beneath the MCU, whereas the two upper parts of the Schrader Bluff Formation, which are separated by a transgressive surface, lie above the MCU (Decker, 2007; fig. 4).

Decker (2007) established a sequence-stratigraphic framework for the Schrader Bluff Formation by principally examining regional subsurface datasets. In light of this work, it became evident that the locally applied informal subdivisions of lower, middle, and upper parts for the Schrader Bluff Formation as proposed and applied by Mull and others (2003, 2004, 2005) do not convey the regional complexity of the formation. Subsequent mapping by Gillis and others (2014), Herriott and others (in preparation), and this study reserve usage of the terms *lower*, *middle*, and *upper* Schrader Bluff Formation to refer to the regional, sequence stratigraphically significant subdivisions of the Schrader Bluff Formation in the sense of Decker (2007). Within this context, we retain the Rogers Creek, Barrow Trail, and Sentinel Hill Members, which are now recognized as the regional lower part of the Schrader Bluff Formation; these members do not occur in outcrop east of the Anaktuvuk River, mainly reflecting basinward facies changes from shelfal Schrader Bluff Formation to deep-water Canning Formation and Hue Shale equivalents that were incised during establishment of the MCU (Decker, 2007). We do not recognize middle or upper Schrader Bluff Formation in the study area. Our intention in re-introducing the older member nomenclature of Detterman and others (1963) and Brosgé and Whittington (1966) for the (lower)

Figure 14. Field photographs of Sentinel Hill Member, Schrader Bluff Formation, at Shivugak Bluff. **A**. View east-northeastward of dominantly Sentinel Hill along west-central part of Shivugak Bluff. See Sentinel Hill Member–Prince Creek Formation contact at red arrows. Topographic relief of bluff is ~120 m, for sense of scale. **B**. Good outcrop expression of thin bedded, Sentinel Hill mudstone and subordinate sandstone that is common to the member but generally renders a recessive weathering profile for the unit. Hammer is 31 cm long. **C**. Detailed view of intercalated mudstone and sandstone of Sentinel Hill. Hammer is 31 cm long. Photographs by T.M. Herriott.

Schrader Bluff Formation of the Umiat–Gubik area is to clearly communicate current understanding of Schrader Bluff Formation stratigraphy.

Detterman and others (1963) reported a 572-m-thick Schrader Bluff Formation along the Chandler River at Tuluvak Bluffs (fig. 1) directly south of the study area. However, approximately 25 km to the north at Shivugak Bluff and the Gubik gas field the Schrader Bluff Formation is thinner at 474 m thick (Brosgé and Whittington, 1966). An even thinner, approximately 320-m-thick Schrader Bluff Formation is identified in the Tulaga 1 well (Decker, 2007), which lies approximately 35 km north-northeast of the Shivugak Bluff/Gubik gas field area. These thicknesses indicate a marked northward thinning of the lower

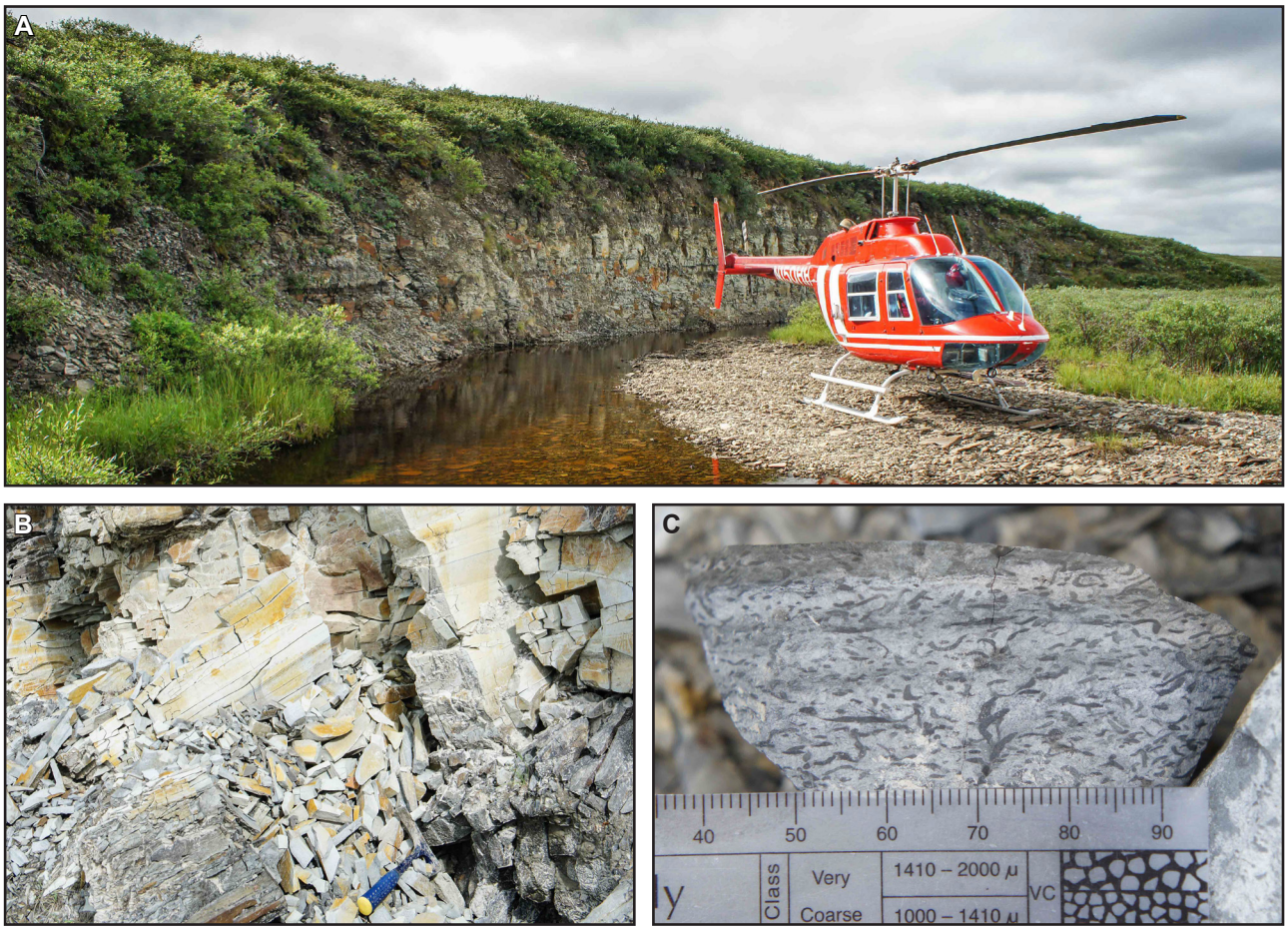

Figure 15. Field photographs of Barrow Trail Member, Schrader Bluff Formation. **A**. Small cutbank exposure of Barrow Trail along an unnamed tributary near the headwaters of Kogosukruk River. This resistant, silicified, thin- to medium-bedded sandstone and siltstone succession is typical of the Barrow Trail (see also fig. 3C). This outcrop lies ~1 km north of the map area. **B**. Blocky to hackly weathering of silicified deposits are common in the unit, and likely reflects a tuffaceous component to these strata. This outcrop is near the mouth of Fossil Creek. Hammer is 31 cm long. **C**. Detailed view of *Phycosiphon* in very fine-grained sandstone. This trace fossil is abundant in Barrow Trail, and is also common in the overlying Sentinel Hill. *Phycosiphon* may constitute the "dark-gray spindle(s)" described by Detterman and others (1963). Rock fragment is from outcrop of figure 3C. Scale in mm. Photographs by T.M. Herriott.

Schrader Bluff Formation, which is reflected on cross section B–B' (sheet 1). A similar pattern and comparable degree of northward thinning of the lower Schrader Bluff stratigraphy is also evident in our examination of an approximately 60-km-long, north-trending seismic line in the Anaktuvuk River area east and northeast of the study area. Future investigations may determine what basin-scale factors controlled this northward thinning trend. Hypotheses that may be tested include 1) whether Santonian–Campanian accommodation increased south of the Barrow arch toward the basin axis as a function of continued compaction of Torok clinoforms; 2) whether a northward decreasing sandstone:shale ratio may have rendered a thinner lower Schrader Bluff succession to the north that would also have been subjected to greater compaction during burial; and/or 3) whether foreland basin flexural subsidence continued during the Late Cretaceous.

Note that the Schrader Bluff members described below typically express a predictable weathering profile, with Rogers Creek and Sentinel Hill Members generally being recessive, muddier units that underlie and overlie, respectively, the commonly more resistant, sandier Barrow Trail Member.

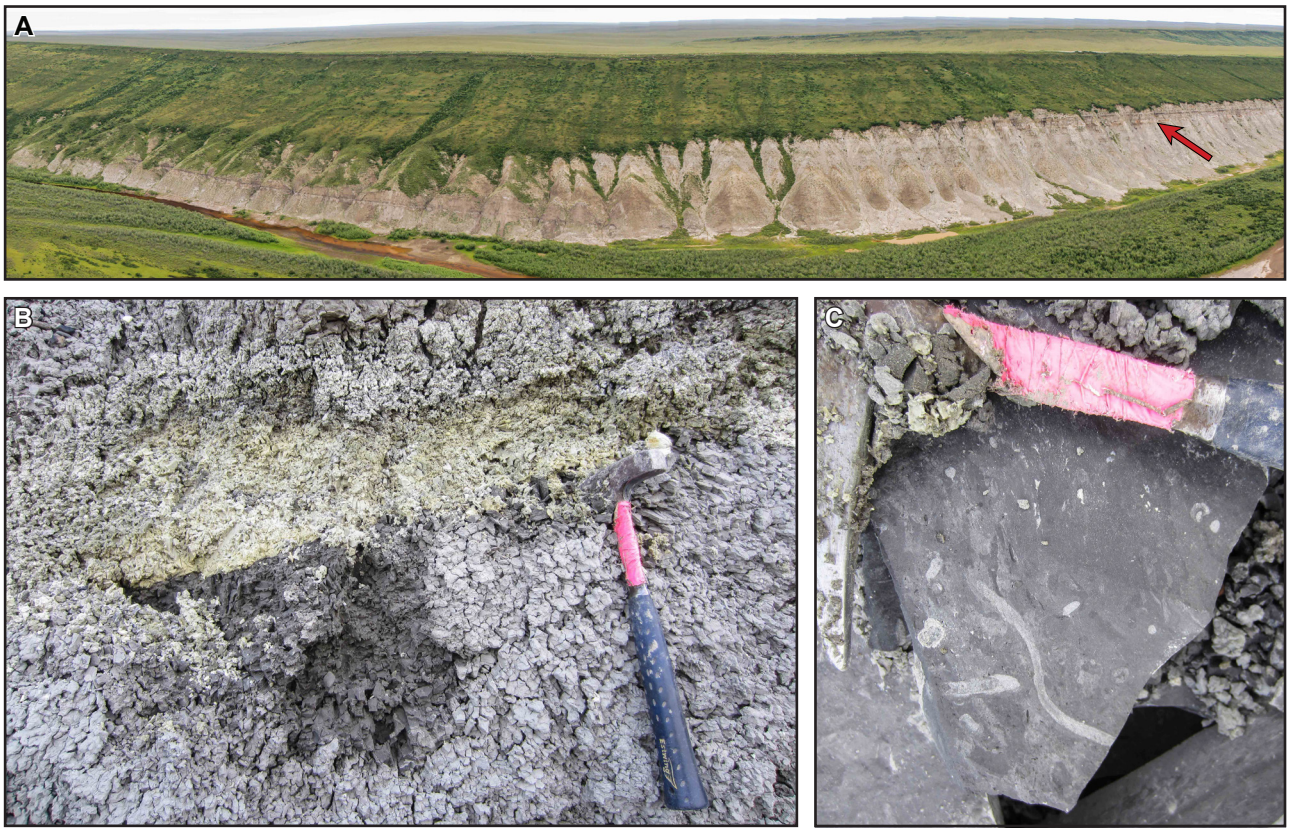

Figure 16. Field photographs of Rogers Creek Member, Schrader Bluff Formation. **A**. Oblique aerial view northwestward of Rogers Creek strata cropping out at the southwestern end of Shivugak Bluff. Contact with overlying Barrow Trail Member marked by the red arrow. Topographic relief of bluff near center of photograph is ~70 m, for sense of scale. Photograph by T.M. Herriott. **B**. The bentonitic, typically fine-grained Rogers Creek forms very few outcrops in the map area, with several small exposures in the Prince Creek drainage (this photograph and C). Note poorly indurated, hackly fracturing character of this generally recessive unit. Pistachio green bentonites (above hammer) are locally observed. Hammer is ~30 cm long. Photograph by D.J. Mauel. **C**. View of well indurated, very fine-grained Rogers Creek sandstone with discrete, light-gray trace fossils (*Planolites[?]*). Specimen is from same locality as B. Hammer for sense of scale. Photograph by D.J. Mauel.

Ksbls SCHRADER BLUFF FORMATION, REGIONAL LOWER PART, SENTINEL HILL MEMBER (middle Santonian–early Campanian: Jones and Gryc, 1960; Detterman and others, 1963; Brosgé and Whittington, 1966) (mapped in the sense of Detterman and others, 1963; Brosgé and Whittington, 1966)—Brown to light- to dark-gray, locally distinctly brown- and brown-purple-weathering, chiefly thin-bedded, moderately to poorly indurated, tuffaceous to locally siliceous, faintly ripple cross-laminated to wispy, disrupted, or convolute laminated mudstone and very fine-grained sandstone, with subordinate light-gray- to brown-purple-weathering, plane-laminated to ripple cross-laminated to locally trough cross-stratified, very fine-grained sandstone in amalgamated bedsets to 10 m thick. Recessive intervals are common, comprising "popcorn"-weathering, light- to dark-gray, bentonitic claystone and yellow-green to pistachio-lime-colored bentonite. Amalgamated sandstone lithofacies contains thin lag deposits of intra-formational mudstone rip-up clast conglomerates, with laminae defined by carbonaceous debris and rhizoliths locally observed. Trace fossil assemblage commonly includes *Schaubcylindrichnus*, *Paleophycos*, and locally densely

packed *Phycosiphon*. Shell fragments from large *Sphenoceramus* are locally observed. Member is 119 m thick near Shivugak Bluff (Brosgé and Whittington, 1966).

Ksblb SCHRADER BLUFF FORMATION, REGIONAL LOWER PART, BARROW TRAIL MEMBER (middle Santonian–early Campanian: Jones and Gryc, 1960; Detterman and others, 1963; Brosgé and Whittington, 1966) (mapped in the sense of Detterman and others, 1963; Brosgé and Whittington, 1966)—Light-gray to tan to brown, thin- to medium-bedded, typically well indurated, locally friable, low-angle wavy, trough, hummocky, and swaley cross-stratified, locally argillaceous, locally carbonaceous and woody debris-bearing, tuffaceous, erosionally resistant very fine- to fine-grained sandstone, with subordinate gray, medium- to thick-bedded, carbonaceous mudstone, dark-gray to black, thin-bedded, siliceous tuff, and chocolate-brown to olive-green, medium-bedded, "popcorn"-weathering bentonitic tuff. Sandstone beds are locally ripple cross-laminated and locally exhibit sharp, scoured bases with up to 80 cm of erosional relief. Siderite nodule, sandstone rip-up clast, and extra-basinal clast conglomerates occur as thin lag deposits. Sandstone and mudstone beds are locally bioturbated, and discrete trace fossils include *Macaronichnus*, *Asterosoma*, and *Schaubcylindrichnus*; a medium- to dark-gray, hackly weathering, well indurated very fine-sandstone and mudstone lithofacies distinctly occurs in this unit and is commonly intensely bioturbated by *Phycosiphon*. Prismatic calcite detritus, likely from *Inoceramus* shells, is locally abundant, as are partially preserved *Sphenoceramus* specimens. Member is 175 m thick at Shivugak Bluff (Brosgé and Whittington, 1966).

Ksblr SCHRADER BLUFF FORMATION, REGIONAL LOWER PART, ROGERS CREEK MEMBER (middle Santonian–early Campanian: Jones and Gryc, 1960; Detterman and others, 1963; Brosgé and Whittington, 1966) (mapped in the sense of Detterman and others, 1963; Brosgé and Whittington, 1966)—Light- to dark-gray to olive-brown, thin- to medium-bedded, typically poorly indurated, tuffaceous to bentonitic, ripple cross-laminated to structureless siltstone and mudstone, with subordinate light-gray- to light-tan-weathering, locally thick-bedded, tuffaceous, ripple cross-laminated, locally well developed hummocky and swaley cross-stratified, coarsening and thickening upward packages of very fine- to fine-grained sandstone. Distinctive light-yellow- to white-weathering, very well indurated, siliceous tuff beds locally observed, as are rare, buff-weathering, very well indurated limestone beds with a probable siliciclastic constituent. Recessive intervals are common and inferred to contain abundant bentonite based on "popcorn"-weathering of colluvium. *Skolithos* traces and *Sphenoceramus* body fossils are observed in the sandstone facies. Member is 178–181 m thick in Gubik Test Nos. 1 and 2 (Robinson, 1958; Brosgé and Whittington, 1966).

TULUVAK FORMATION (regionally Turonian–Coniacian: see review by Mull and others, 2003; potentially as old as Cenomanian: Shimer and others, 2016) (defined and/or locally mapped by Gryc and others, 1951; Whittington, 1956; Detterman and others, 1963; Brosgé and Whittington, 1966; revised by Mull and others, 2003)—The Tuluvak Formation (fig. 17) is a regionally regressive, locally very coarse-grained nonmarine and shallow-marine (nearshore) sandstone and conglomerate unit correlative with principally offshore to deep-water facies of Seabee Formation (Houseknecht and Schenk, 2005; Decker, 2007) (fig. 4). Mull and others (2003)

reported that the most basinward outcrops of the Tuluvak are in the Umiat (Mull and others, 2004) and Chandler Lake (Kelley, 1990) Quadrangles and suggested that the terminal shelf margin of the Tuluvak–Seabee depositional cycle may lie in the western Sagavanirktok Quadrangle (>40 km east of study area). Houseknecht and Schenk (2005) interpreted the lower Tuluvak at the eastern extent of Umiat Mountain as chiefly recording progradational delta front and channel associated processes; this locality is the best exposure in the map area to examine Tuluvak (fig. 17). The revised Tuluvak Formation (see Mull and others, 2003) in the Umiat–Gubik area is approximately 285 m thick (Robinson; 1958; Molenaar, 1982) and serves as the primary reservoir of natural gas at the Gubik field (see above). Tuluvak sandstones near the summit of Umiat Mountain emit a slight, ephemeral hydrocarbon odor.

Figure 17. Field photographs of Tuluvak Formation at Umiat Mountain. **A.** Oblique aerial view northwestward of erosionally resistant Tuluvak overlying generally recessive Seabee Formation, with the Colville River in the foreground; the Seabee–Tuluvak contact is marked by the red arrow. Stark juxtaposition of disparate Seabee facies in outcrop below the heavily vegetated draw at left of photograph delineates the normal fault mapped on sheet 1 (see also Houseknecht and Schenk, 2005). The Umiat Mountain summit lies at the leftmost skyline, ~185 m above the river, for sense of scale. Photograph by M.A. Wartes. **B.** Tabular, very thick- to thin-bedded, graded sandstones at the base of Tuluvak immediately above river level in A. Hammer is ~30 cm long (see magenta outline). Photograph by R.J. Gillis. **C.** Detailed character of salt-and-pepper colored sandstone in float near the lower Tuluvak. This bedding plane hosts abundant cm-scale coalified plant fragments, which are locally common in Tuluvak. Marker is 14 cm long. Photograph by M.A. Wartes.

Ktu TULUVAK FORMATION (locally Turonian–Coniacian: Jones and Gryc, 1960; Detterman and others, 1963; Brosgé and Whittington, 1966; potentially as old as Cenomanian: Shimer and others, 2016)—Tan- to brown- to orange-brown-weathering, medium-gray to medium-brown, chiefly thin- to medium-bedded, commonly normally graded, well indurated, moderately-sorted, lithic- and locally quartz-rich, locally carbonaceous (including coalified woody debris), erosionally resistant very fine- to medium-grained sandstone, with subordinate thin-bedded, plane-parallel laminated mudstone. Sandstone grains are subrounded to subangular. Mudstone rip-up clasts and siderite nodules as clasts are locally observed in sandstone beds, as are symmetrical ripples and low angle cross-stratification.

SEABEE FORMATION (regionally Cenomanian–Coniacian: Gryc and Jones, 1960; Lanphere and Tailleur, 1983; see review by Mull and others, 2003; see also Shimer and others, 2016) (defined and/or locally mapped by Gryc and others, 1951; Whittington, 1956; Detterman and others, 1963; Brosgé and Whittington, 1966; revised by Mull and others, 2003, 2004)—The Seabee Formation (fig. 18) principally consists of transgressive and regressive offshore to deep-marine strata of the Tuluvak–Seabee depositional cycle (Houseknecht and Schenk, 2005; Decker, 2007) (fig. 4). The lower Seabee Formation in the Umiat–Gubik and surrounding areas comprises deposits that draped the relict, broad Nanushuk shelf during a major transgression that terminated Nanushuk–Torok deposition (Molenaar, 1985, 1988; Bird and Molenaar, 1992; Houseknecht and Schenk, 2005; Decker, 2007; Houseknecht and others, 2009; LePain and others, 2009); this transgression resulted in a regional-scale westward shift of the paleoshoreline to hundreds of kilometers west of Umiat (Houseknecht and Schenk, 2005; Decker, 2007). The basal Seabee transgressive succession is overlain by shelf-perched, prodelta-associated Seabee clinoforms that prograded basinward of coeval nearshore and nonmarine strata of the Tuluvak Formation with an ultimate shelf margin established east of the mapped area (Houseknecht and Schenk, 2005; see reference and below for additional, higher-frequency sequence-stratigraphic relations within Seabee). The inherited shelf–slope–basin floor profile strongly influenced the stratigraphic architecture of the Seabee Formation, yielding lower-relief (hundreds of feet) prodelta Seabee clinoforms above the Nanushuk paleoshelf and higher-relief (thousands of feet) slope clinoforms to the east of the terminal Nanushuk–Torok shelf margin that lies approximately 20 km east of the study area (Houseknecht and Schenk, 2005; Decker, 2007; see below).

Houseknecht and Schenk (2005) provided a sequence-stratigraphic framework for the upper Nanushuk–Seabee–lower Tuluvak stratigraphy at Umiat Mountain, interpreting distal offshore environments for the bulk of Seabee, although an intra-Seabee lowstand systems tract notably hosts a 37-m-thick sandy shoreface succession encased in hundreds of meters of transgressive and highstand bentonitic mudstone. Reported thicknesses for the revised Seabee Formation (Mull and others, 2003) range from 365–440 m in the Umiat–Gubik area (Collins, 1958; Robinson, 1958; Molenaar, 1982), but the unit regionally thickens markedly basinward as noted above. The south face of Umiat Mountain includes an oil-stained outcrop of Seabee sandstone (Houseknecht and Schenk, 2005) and is the only locality in the map area where the formation is well exposed (figs. 17A and 18).

Ks SEABEE FORMATION (locally Cenomanian–Turonian: Jones and Gryc, 1960; Lanphere and Tailleur, 1983; Shimer and others, 2016)—Tan-gray- to medium-gray-weathering, medium- to dark-gray, thin-bedded, dominantly poorly indurated, tuffaceous to bentonitic, locally fissile, plane-parallel laminated to rippled siltstone, mudstone, shale, and claystone, with subordinate tan-gray-weath-

Figure 18. Field photographs of Seabee Formation at Umiat Mountain. **A.** View east-southeastward of mostly dark-gray-weathering Seabee exposed in the southwest-facing aspect of Umiat Mountain. The Seabee–Tuluvak contact is marked by red arrows. See figure 17A for a different perspective of this bluff. Geologist standing at lower left of photograph, for sense of scale. **B.** Thick sandstone beds are locally observed in the Seabee, which is dominantly bentonitic mudstone and shale that are mainly poorly exposed. Distant outcrop along point at river level is the same as in A. Mattock is ~65 cm long. **C.** Detailed view of very thinly bedded, fissile character of commonly bentonitic strata in the Seabee. Marker is 14 cm long. Photographs by M.A. Wartes.

ering, medium-gray, thin- to very thick-bedded, locally well indurated, commonly normally graded, low-angle cross-stratified (for example, hummocky, swaley, and irregularly) very fine-grained sandstone. Discrete, very thin-bedded bentonite hori-

zons are common, and mudrock-dominated zones in the Seabee are typically covered in bentonitic slope wash that exhibits a characteristic "popcorn"-weathering style. *Inoceramus* shells, shell fragments, and prismatic calcite detritus are locally observed.

NANUSHUK FORMATION (regionally Albian–Cenomanian: Ahlbrandt and others, 1979; Huffman and others, 1985, 1988; LePain and others, 2009; Shimer and others, 2016; see review by Mull and others, 2003) (defined and/or locally mapped by Schrader, 1902; Gryc and others, 1951; Detterman, 1956b; Detterman and others, 1963; Brosgé and Whittington, 1966; revised by Mull and others, 2003, 2004)—The Nanushuk Formation (fig. 19) regionally records nonmarine and shallow-marine topset depositional systems that interfingered with slope foreset environments of the time-equivalent Torok Formation (Molenaar, 1985, 1988; Bird, 2001b; LePain and Kirkham, 2001; Houseknecht and Schenk, 2005; Decker, 2007; LePain and others, 2009) (fig. 4). Although the Torok does not crop out in the map area, it plays an important role in the study area's style of deformation and petroleum geology (see above). Houseknecht and Schenk (2005) mapped in the subsurface the ultimate (most basinward) Nanushuk–Torok shelf margin approximately 60 km east of Umiat (~20 km east of map area), where this important paleobathymetric element is north-trending and east-facing. Deposition of the uppermost Nanushuk (Ninuluk Formation of former usage; see revision by Mull and others, 2003) coincided with a basin-wide transgression (Detterman and others, 1963; Huffman and others, 1985, 1988), rendering retrogradational stacking of smaller-scale progradational packages of the youngest Nanushuk strata (LePain and others, 2009) as depositional systems backstepped to the west (Houseknecht and Schenk, 2005; Shimer and others, 2014). The larger-scale transgression ultimately terminated the Nanushuk–Torok depositional cycle and yielded the basal transgressive Seabee Formation as described above.

Detailed sedimentologic work at Umiat Mountain (Houseknecht and Schenk, 2005) and the Colville incision locality (LePain and others, 2009) indicates that the upper Nanushuk of the study area records estuarine and shoreface sedimentation as well as fluvial processes. These reports are consistent with recent examination of Umiat oil field cores by Shimer and others (2014), who interpreted the Ninuluk as mainly reflecting retrogradational stacking of deltaic and shoreface deposits.

The Nanushuk in the Umiat and Gubik fields is reported to be 300–330 m thick (Collins, 1958; Robinson, 1958; Molenaar, 1982), although the unit thickens markedly to the south and west (Bird, 1988c). The Nanushuk thins to zero depositional thickness to the east at the aforementioned terminal Nanushuk–Torok shelf margin. Nanushuk outcrops in the mapped area mostly correspond to the Ninuluk Formation of former usage (see Mull and others, 2003). Good exposures of these rocks occur along the western extent of the south face of Umiat Mountain, where some sandstone beds are oil saturated (Houseknecht and Schenk, 2005) and probably associated with seeps near the bank of the Colville River. The Colville incision also permits examination of the uppermost Nanushuk Formation (see LePain and others, 2009; fig. 19). Older (Albian) Nanushuk sandstones host the main hydrocarbon accumulation at the Umiat field (Molenaar, 1982; Shimer and others, 2014; Hanks and others, 2014; this study), which is the only proven oil field in the Brooks Range foothills (see above).

Kn NANUSHUK FORMATION (locally Cenomanian: see Houseknecht and Schenk, 2005; LePain and others, 2009; see also Shimer and others, 2016; Albian to Cenomanian in the subsurface: see Molenaar, 1982)—Tan- to gray-brown- to rusty-brown-weathering, medium-gray to light-brown to gray-brown, thick- to very thick-bedded, dominantly well indurated, commonly normally graded, locally structureless but commonly trough, hummocky, swaley, or tabular (planar and tangential) cross-stratified, chiefly fine- to

Figure 19. Field photographs of Nanushuk Formation at the Colville incision locality. **A.** Oblique aerial view northward of the uppermost nearly 100 m of the Nanushuk Formation (see LePain and others, 2009). Seabee Formation is mapped at and beyond the top of the bluff. Outcrop extends for ~1 km along river and topographic relief of bluff near center of photograph is ~45 m, for sense of scale. Prominent barrel distortion of image is a perspective effect of stitching numerous photographs together to compose the panorama. **B.** Typical outcrop character of thick-bedded, structureless to cross-stratified sandstone of the Nanushuk Formation. Hammer is 31 cm long. **C.** Highly fossiliferous horizons are commonly associated with pebbly lag deposits in marine (probably shoreface) sandstones at this locality (see LePain and others, 2009). Pencil at rubberized grip is 1.2 cm diameter. Photographs by T.M. Herriott.

medium-grained sandstone. The fine- to medium-grained sandstone lithofacies is commonly overlain by subordinate dark-gray- to gray-brown- to light-rusty-brown-weathering, medium-gray to tan-gray to tan, very thin- to thin-bedded, moderately well indurated, ripple to low-angle cross-laminated to plane-parallel laminated very fine-grained sandstone and mudstone. Centimeter-scale, coalified wood fragments and very thin pebbly lags are locally observed.

ACKNOWLEDGMENTS

The State of Alaska funded this study, with additional support from the U.S. Geological Survey's National Cooperative Geologic Mapping Program (STATEMAP award number G12AC20187). Work by, and discussions with, Gil Mull, Dave LePain, and Dave Houseknecht were invaluable to this study. Ken Helmold, Dolores van der Kolk, Grant Shimer, Pete Flaig, Julie Houle, Meg Kramer, and Don Krouskop also shared their knowledge of the Umiat–Gubik area. Richard Kemnitz provided many insights regarding field logistics. Our field camps at Umiat were operated by Horst Expediting and 70 North. Helicopter pilot Tom "Rat" Ratledge safely transported the crew during field campaigns. Trish Ekberg, Nina Harun, and Mike Hendricks served additional geographic information system (GIS) support. Simone Montayne managed metadata for this report. Kristen Janssen provided manuscript formatting and layout. We thank Dave LePain and Tom Homza for thorough reviews that improved the clarity and content of this paper.

REFERENCES

Ahlbrandt, T.S., 1979, Introduction to geologic studies of the Nanushuk Group, North Slope, Alaska, *in* Ahlbrandt, T.S., ed., Preliminary geologic, petrologic, and paleontologic results of the study of Nanushuk Group rocks, North Slope, Alaska: U.S. Geological Survey Circular 794, p. 1–4.

Ahlbrandt, T.S., Huffman, A.C., Jr., Fox, J.E., and Pasternack, Ira, 1979, Depositional framework and reservoir-quality studies of selected Nanushuk Group outcrops, North Slope, Alaska, *in* Ahlbrandt, T.S., ed., Preliminary geologic, petrologic, and paleontologic results of the study of Nanushuk Group rocks, North Slope, Alaska: U.S. Geological Survey Circular 794, p. 14–31.

Allmendinger, R.W., Cardozo, Nestor, and Fisher, D.M., 2013, Structural Geology Algorithms: Vectors and Tensors: Cambridge University Press, Cambridge, England, 289 p.

Bailey, Alan, 2016, The headache of low oil flow through TAPS: Petroleum News, v. 21, no. 6, p. 7.

Biddle, K.T., and Christie-Blick, Nicholas, 1985, Glossary—Strike-slip deformation, basin formation, and sedimentation, *in* Biddle, K.T., and Christie-Blick, Nicholas, eds., Strike-slip deformation, basin formation, and sedimentation: Society of Economic Paleontologists and Mineralogists Special Publication No. 37, p. 375–386. https://doi.org/10.2110/pec.85.37.0361

Bird, K.J., 1981, Petroleum exploration of the North Slope in Alaska, U.S.A.: U.S. Geological Survey Open-File Report 81-227, 43 p.

———1988a, The geologic basis for appraising undiscovered hydrocarbon resources in the National Petroleum Reserve in Alaska by the play-appraisal method, *in* Gryc, George, ed., Geology and exploration of the National Petroleum Reserve in Alaska, 1974 to 1982: U.S. Geological Survey Professional Paper 1399, p. 81–116.

———1988b, Alaskan North Slope stratigraphic nomenclature and data summary for government-drilled wells, *in* Gryc, George, ed., Geology and exploration of the National Petroleum Reserve in Alaska, 1974 to 1982: U.S. Geological Survey Professional Paper 1399, p. 317–355.

———1988c, Structure-contour and isopach maps of the National Petroleum Reserve in Alaska, *in* Gryc, George, ed., Geology and exploration of the National Petroleum Reserve in Alaska, 1974 to 1982: U.S. Geological Survey Professional Paper 1399, p. 355–377.

———2001a, Alaska: A twenty-first-century petroleum province, *in* Downey, M.W., Threet, J.C., and Morgan, W.A., eds., Petroleum provinces of the twenty-first century: American Association of Petroleum Geologists Memoir 74, p. 137–165.

———2001b, Framework geology, petroleum systems, and play concepts of the National Petroleum Reserve—Alaska, *in* Houseknecht, D.W., ed., Petroleum plays and systems in the National Petroleum Reserve—Alaska: SEPM (Society for Sedimentary Geology) Core Workshop 21, p. 5–17. https://doi.org/10.2110/cor.01.01.0005

Bird, K.J., and Bader, J.W., 1987, Regional geologic setting and history of petroleum exploration, *in* Bird, K.J., and Magoon, L.B., eds., Petroleum geology of the northern part of the Arctic National Wildlife Refuge, northeastern Alaska: U.S. Geological Survey Bulletin 1778, p. 17–25.

Bird, K.J., and Houseknecht, D.W., 2011, Geology and petroleum potential of the Arctic Alaska petroleum province, *in* Spencer, A.M., Embry, A.F., Gautier, D.L., Stoupakova, A.V., and Sørensen, Kai, eds., Arctic petroleum geology: Memoirs of the Geological Society of London, v. 35, ch. 32, p. 485–499. https://doi.org/10.1144/M35.32

Bird, K.J., and Molenaar C.M., 1992, The North Slope foreland basin, *in* Macqueen, R.W., and Leckie, D.A., eds., Foreland basins and foldbelts: American Association of Petroleum Geologists Memoir 55, p. 363–393.

Blythe, A.E., Bird, J.M., and Omar, G.I., 1996, Deformational history of the central Brooks Range, Alaska—Results from fission-track and $^{40}Ar/^{39}Ar$ analyses: Tectonics, v. 15, p. 440—455. http://dx.doi.org/10.1029/95TC03053

Brooks, A.H., 1916, The Alaskan mining industry in 1915, in U.S. Geological Survey, Mineral resources of Alaska, report on progress of investigations in 1915: U.S. Geological Survey Bulletin 642, p. 16–72.

Brosgé, W.P., and Whittington, C.L., 1966, Geology of the Umiat–Maybe Creek region, Alaska: U.S. Geological Survey Professional Paper 303-H, p. 501–638.

Cardozo, Nestor, and Allmendinger, R.W., 2013, Spherical projections with OSXStereonet: Computers & Geosciences, v. 51, p. 193–205. https://doi.org/10.1016/j.cageo.2012.07.021

Carter, L.D., and Galloway, J.P., 1986, Engineering-geologic maps of northern Alaska, Umiat Quadrangle: U.S. Geological Survey Open-File Report 86-335, 2 sheets, scale 1:250,000, 16 p.

Christie-Blick, Nicholas, and Biddle, K.T., 1985, Deformation and basin formation along strike-slip faults, *in* Biddle, K.T., and Christie-Blick, Nicholas, eds., Strike-slip deformation, basin formation, and sedimentation: Society of Economic Paleontologists and Mineralogists Special Publication 37, p. 1–34. https://doi.org/10.2110/pec.85.37.0001

Cole, Frances, Bird, K.J., Toro, Jaime, Roure, François, O'Sullivan, P.B., Pawlewicz, Mark, and Howell, D.G., 1997, An integrated model for the tectonic development of the frontal Brooks Range and Colville basin 250 km west of the Trans-Alaska Crustal Transect: Journal of Geophysical Research, v. 102, p. 20,685–20,708. http://dx.doi.org/10.1029/96JB03670

Collins, F.R., 1958, Test wells, Umiat area, Alaska: U.S. Geological Survey Professional Paper 305-B, 3 sheets, p. 71–206.

Decker, P.L., 2007, Brookian sequence stratigraphic correlations, Umiat Field to Milne Point Field, west-central North Slope, Alaska: Alaska Division of Geological & Geophysical Surveys Preliminary Interpretive Report 2007-2, 1 sheet, 19 p.

———2010, Brookian sequence stratigraphic framework of the northern Colville foreland basin, central North Slope, Alaska (poster and presentation): DNR Spring Technical Review Meeting, Anchorage, April 21–22, 2010: Alaska Division of Geological & Geophysical Surveys, 1 sheet, 30 p.

Decker, P.L., and Wartes, M.A., 2008, Geochemistry of the Aupuk gas seep along the Colville River—Evidence for a thermogenic origin, *in* Wartes, M.A., and Decker, P.L., eds., Preliminary results of recent geologic field investigations in the Brooks Range Foothills and North Slope, Alaska: Alaska Division of Geological & Geophysical Surveys Preliminary Interpretive Report 2008-1E, p. 47–54.

Detterman, R.L., 1956a, New member of Seabee formation, Colville Group, *in* Gryc, George, Bergquist, H.R., Detterman, R.L., Patton, W.W., Jr., Robinson, F.M., Rucker, F.P., and Whittington, C.L., Mesozoic sequence in Colville River region, northern Alaska: American Association of Petroleum Geologists Bulletin, v. 40, no. 2, p. 253–254.

———1956b, New and redefined nomenclature of Nanushuk group, *in* Gryc, George, Bergquist, H.R., Detterman, R.L., Patton, W.W., Jr., Robinson, F.M., Rucker, F.P., and Whittington, C.L., Mesozoic sequence in Colville River region, northern Alaska: American Association of Petroleum Geologists Bulletin, v. 40, no. 2, p. 233–244.

Detterman, R.L., Bickel, R.S., and Gryc, George, 1963, Geology of the Chandler River region, Alaska: U.S. Geological Survey Professional Paper 303-E, p. 223–324.

Division of Oil and Gas, 2008, Regional geology of the North Slope (plate 2 of 4): Alaska Department of Natural Resources, North Slope Resource Series, scale 1:1,000,000.

Flaig, P.P., 2010, Depositional environments of the Late Cretaceous (Maastrichtian) dinosaur-bearing Prince Creek Formation: Colville River region, North Slope, Alaska: University of Alaska Fairbanks, Ph.D. dissertation, 311 p.

Flaig, P.P., Fiorillo, A.R., and McCarthy, P.J., 2014, Dinosaur-bearing hyperconcentrated flows of Cretaceous Arctic Alaska: Recurring catastrophic event beds on a distal paleopolar coastal plain: PALAIOS, v. 29, p. 594–611. https://doi.org/10.2110/palo.2013.133

Flaig, P.P., McCarthy, P.J., and Fiorillo, A.R. 2011, A tidally influenced, high-latitude coastal-plain: The Upper Cretaceous (Maastrichtian) Prince Creek Formation, North Slope, Alaska, *in* Davidson, S.K., Leleu, Sophie, and North, C.P., eds., From river to rock record: The preservation of fluvial sediments and their subsequent interpretation: SEPM (Society for Sedimentary Geology) Special Publication 97, p. 233–264. https://doi.org/10.2110/sepmsp.097.233

———2013, Anatomy, evolution, and paleoenvironmental interpretation of an ancient Arctic coastal plain: Integrated paleopedology and palynology from the Upper Cretaceous (Maastrichtian) Prince Creek Formation, North Slope, Alaska, USA, *in* Driese, S.G., Nordt, L.C., and McCarthy, P.J., eds., New frontiers in paleopedology and terrestrial paleoclimatology: Paleosols and soil surface analog systems: SEPM (Society for Sedimentary Geology) Special Publication 104, p. 179–230. https://doi.org/10.2110/sepmsp.104

Flores, R.M., Myers, M.D., Houseknecht, D.W., Stricker, G.D., Brizzolara, D.W., Ryherd, T.J., and Takahashi, K.I., 2007a, Stratigraphy and facies of Cretaceous Schrader Bluff and Prince Creek Formations in Colville River Bluffs, North Slope, Alaska: U.S. Geological Survey Professional Paper 1748, 45 p.

Flores, R.M., Stricker, G.D., Decker, P.L., and Myers, M.D., 2007b, Sentinel Hill core test 1—Facies descriptions and stratigraphic reinterpretations of the Prince Creek and Schrader Bluff Formations, North Slope, Alaska: U.S. Geological Survey Professional Paper 1747, 34 p.

Garrity, C.P., Houseknecht, D.W., Bird, K.J., Potter, C.J., Moore, T.E., Nelson, P.H., and Schenk, C.J., 2005, U.S. Geological Survey 2005 oil and gas resource assessment of the central North Slope, Alaska—Play maps and results: U.S. Geological Survey Open-File Report 2005-1182, 1 p.

Gillis, R.J., Decker, P.L., Wartes, M.A., Loveland, A.M., and Hubbard, T.D., 2014, Geologic map of the south-central Sagavanirktok Quadrangle, North Slope, Alaska: Alaska Division of Geological & Geophysical Surveys Report of Investigation 2014-4, 2 sheets, scale 1:63,360, 24 p.

Grantz, Arthur, Dinter, D.A., and Biswas, N.N., 1983, Map, cross sections, and chart showing late Quaternary faults, folds, and earthquake epicenters on the Alaskan Beaufort shelf: U.S. Geological Survey Miscellaneous Investigations Series Map I-1182-C, 3 sheets, scale 1:500,000, 7 p.

Grantz, Arthur, May, S.D., and Hart, P.E., 1990, Geology of the Arctic continental margin of Alaska, *in* Grantz, Arthur, Johnson, Leonard, and Sweeney, J.F., eds., The Arctic Ocean region: The Geology of North America, Geological Society of America, Boulder, Colorado, v. L, ch. 16, p. 257–288. https://doi.org/10.1130/DNAG-GNA-L.257

Gryc, George, 1956, Introduction and summary, in Gryc, George, Bergquist, H.R., Detterman, R.L., Patton, W.W., Jr., Robinson, F.M., Rucker, F.P., and Whittington, C.L., Mesozoic sequence in Colville River region, northern Alaska: American Association of Petroleum Geologists Bulletin, v. 40, no. 2, p. 209–214.

Gryc, George, ed., 1988, Geology and exploration of the National Petroleum Reserve in Alaska, 1974 to 1982: U.S. Geological Survey Professional Paper 1399, 940 p.

Gryc, George, Bergquist, H.R., Detterman, R.L., Patton, W.W., Jr., Robinson, F.M., Rucker, F.P., and Whittington, C.L., 1956, Mesozoic sequence in Colville River region, northern Alaska: American Association of Petroleum Geologists Bulletin, v. 40, no. 2, p. 209–254.

Gryc, George, Patton, W.W., Jr., and Payne, T.G., 1951, Present Cretaceous stratigraphic nomenclature of northern Alaska: Washington Academy of Sciences Journal, v. 41, no. 5, p.159–167.

Hanks, C.L., Shimer, Grant, Kohshour, Iman Oraki, Ahmadi, Mohabbat, McCarthy, P.J., Dandekar, Abhijit, Mongrain, Joanna, Wentz, Raelene, 2014, Integrated reservoir characterization and simulation of a shallow, light-oil, low-temperature reservoir: Umiat field, National Petroleum Reserve, Alaska: American Association of Petroleum Geologists Bulletin, v. 98, p. 563–585. https://doi.org/10.1306/08201313011

Harding, T.P., and Lowell, J.D., 1979, Structural styles, their plate-tectonic habitats, and hydrocarbon traps in petroleum provinces: American Association of Petroleum Geologists Bulletin, v. 63, p. 1,016–1,058.

Herriott, T.M., and others, in preparation, Geologic map of the Gilead Creek area, northeastern Brooks Range, Alaska: Alaska Division of Geological & Geophysical Surveys Report of Investigation.

Houseknecht, D.W., and Bird, K.J., 2006, Oil and gas resources of the Arctic Alaska petroleum province, *in* Haeussler, P.J., and Galloway, J.P., eds., Studies by the U.S. Geological Survey in Alaska, 2005: U.S. Geological Survey Professional Paper 1732-A, 11 p.

Houseknecht, D.W., Bird, K.J., and Schenk, C.J., 2009, Seismic analysis of clinoform depositional sequences and shelf-margin trajectories in Lower Cretaceous (Albian) strata, Alaska North Slope: Basin Research, v. 21, p. 644–654. http://dx.doi.org/10.1111/j.1365-2117.2008.00392.x

Houseknecht, D.W, and Schenk, C.J., 2001, Depositional sequences and facies in the Torok Formation, National Petroleum Reserve—Alaska (NPRA), *in* Houseknecht, D.W., ed., Petroleum plays and systems in the National Petroleum Reserve—Alaska: SEPM (Society for Sedimentary Geology) Core Workshop 21 p. 179–199. https://doi.org/10.2110/cor.01.01.0179

———2005, Sedimentology and sequence stratigraphy of the Cretaceous Nanushuk, Seabee, and Tuluvak Formations exposed on Umiat Mountain, north-central Alaska: U.S. Geological Survey Professional Paper 1709-B, 18 p.

Hubbard, R.J., Edrich, S.P., and Rattey, R.P., 1987, Geologic evolution and hydrocarbon habitat of the Arctic Alaska microplate, *in* Tailleur, I.L., and Weimer, Paul, eds., Alaskan North Slope geology: Society of Economic Paleontologists and Mineralogists, Pacific Section, and Alaska Geological Society, Book 50, v. 2, p. 797–830.

Huffman, A.C., ed., 1985, Geology of the Nanushuk Group and related rocks, North Slope, Alaska: U.S. Geological Survey Bulletin 1614, 129 p.

Huffman, A.C., Jr., Ahlbrandt, T.S., and Bartsch-Winkler, Susan, 1988, Sedimentology of the Nanushuk Group, North Slope, *in* Gryc, George, ed., Geology and exploration of the National Petroleum Reserve in Alaska, 1974 to 1982: U.S. Geological Survey Professional Paper 1399, p. 281–298.

Huffman, A.C., Ahlbrandt, T.S., Pasternack, Ira, Stricker, G.D., and Fox, J.E., 1985, Depositional and sedimentologic factors affecting the reservoir potential of the Cretaceous Nanushuk Group, central North Slope, *in* Huffman, A.C., ed., Geology of the Nanushuk Group and related rocks, North Slope, Alaska: U.S. Geological Survey Bulletin 1614, p. 61–74.

Jones, D.L., and Gryc, George, 1960, Upper Cretaceous pelecypods of the genus Inoceramus from northern Alaska: U.S. Geological Survey Professional Paper 334-E, p. 149–165.

Kelley, J.S., 1990, Generalized geologic map of the Chandler Lake Quadrangle, north-central Alaska: U.S. Geological Survey Miscellaneous Field Studies Map 2144-A, 1 sheet, scale 1:250,000, 19 p.

Kirschner, C.E., and Rycerski, B.A., 1988, Petroleum potential of representative stratigraphic and structural elements in the National Petroleum Reserve in Alaska, *in* Gryc, George, ed., Geology and exploration of the National Petroleum Reserve in Alaska, 1974 to 1982: U.S. Geological Survey Professional Paper 1399, p. 191–208.

Kopf, R.W., 1970, Geologic names in use north of the Brooks Range, Alaska, *in* Adkison, W.L., and Brosgé, M.M., eds., Proceedings of the geologic seminar on the North Slope of Alaska: American Association of Petroleum Geologists, Pacific Section, p. Q1–Q5.

Kornbrath, R.W., Myers, M.D., Krouskop, D.L., Meyer, J.F., Houle, J.A., Ryherd, T.J., and Richter, K.N., 1997, Petroleum potential of the eastern National Petroleum Reserve—Alaska: Alaska Department of Natural Resources, Division of Oil and Gas, 30 p.

Kumar, Naresh, Bird, K.J., Nelson, P.H., Grow, J.A., and Evans, K.R., 2002, A digital atlas of hydrocarbon accumulations within and adjacent to the National Petroleum Reserve—Alaska (NPRA): U.S. Geological Survey Open-File Report 2002-71, 80 p.

Lanphere, M.A., and Tailleur, I.L., 1983, K–Ar ages of bentonites in the Seabee Formation, northern Alaska: A Late Cretaceous (Turonian) time-scale point: Cretaceous Research, v. 4, p. 361–370. https://doi.org/10.1016/S0195-6671(83)80004-4

Leffingwell, E. de K., 1919, The Canning River region, northern Alaska: U.S. Geological Survey Professional Paper 109, 6 sheets, various scales, 251 p.

LePain, D.L., and Kirkham, R.A., 2001, Potential reservoir facies in the Nanushuk Formation (Albian–Cenomanian), central North Slope, Alaska: Examples from outcrop and core, *in* Houseknecht, D.W., ed., Petroleum plays and systems in the National Petroleum Reserve—Alaska: SEPM (Society for Sedimentary Geology) Core Workshop 21, p. 19–36. https://doi.org/10.2110/cor.01.01.0019

LePain, D.L., McCarthy, P.J., and Kirkham, Russell, 2009, Sedimentology and sequence stratigraphy of the middle Albian–Cenomanian Nanushuk Formation in outcrop, central North Slope, Alaska: Alaska Division of Geological & Geophysical Surveys Report of Investigation 2009-1, 1 sheet. 78 p.

Lerand, M., 1973, Beaufort Sea, *in* McCrossam, R.G., ed., The future petroleum provinces of Canada—Their geology and potential: Canadian Society of Petroleum Geology Memoir 1, p. 315–386.

Lidji, Eric, 2012, Umiat reserves saga: Petroleum News, v. 17, no. 36, p. 1 and 15.

———2015a, Linc outlines Umiat: Petroleum News, v. 20, no. 25, p. 1 and 19.

———2015b, New Umiat report drops reserves, lowers recoverable based on price: Petroleum News, v. 20, no. 51, p.1 and 15.

———2016, Market challenges two Linc Energy projects: The Explorers, Petroleum News, v. 21, no. 21, p. 53–54.

Magoon, L.B., III, 1994, Petroleum resources in Alaska, *in* Plafker, George, and Berg, H.C., eds., The Geology of Alaska: The Geology of North America, Geological Society of America, Boulder, Colorado, v. G-1, ch. 30, p. 905–936. https://doi.org/10.1130/DNAG-GNA-G1.905

Magoon, L.B., and Bird, K.J., 1985, Alaskan North Slope petroleum geochemistry for the Shublik Formation, Kingak Shale, pebble shale unit, and Torok Formation, in Magoon, L.B., and Claypool, G.E., eds., Alaska North Slope oil/rock correlation study: American Association of Petroleum Geologists Studies in Geology 20, p. 31–48.

Magoon, L.B., Lillis, P.G., Bird, K.J., Lampe, C., and Peters, K.E., 2003, Alaskan North Slope petroleum systems: U.S. Geological Survey Open-File Report 2003-324, 3 sheets.

Marrett, R.A., and Allmendinger, R.W., 1990, Kinematic analysis of fault-slip data: Journal of Structural Geology, v. 12, p. 973–986. https://doi.org/10.1016/0191-8141(90)90093-E

Mayfield, C.F., Tailleur, I.L., and Ellersieck, Inyo, 1988, Stratigraphy, structure, and palinspastic synthesis of the western Brooks Range, northwestern Alaska, *in* Gryc, George, ed., Geology and exploration of the National Petroleum Reserve in Alaska, 1974 to 1982: U.S. Geological Survey Professional Paper 1399, 4 sheets, p. 143–186.

McClay, K.R., 1987, The Mapping of Geological Structures: John Wiley & Sons, Chichester, 161 p.

Miller, E.L., and Hudson, T.L., 1991, Mid-Cretaceous extensional fragmentation of a Jurassic–Early Cretaceous compressional orogen, Alaska: Tectonics, v. 10, p. 781–796. http://dx.doi.org/10.1029/91TC00044

Molenaar, C.M., 1982, Umiat field, an oil accumulation in a thrust-faulted anticline, North Slope of Alaska, *in* Powers, R.B., ed., Geologic studies of the Cordilleran thrust belt: Rocky Mountain Association of Geologists, p. 537–548.

Molenaar, C.M., 1983, Depositional relations of Cretaceous and lower Tertiary rocks, northeastern Alaska: American Association of Petroleum Geologists Bulletin, v. 67, p. 1,066–1,080.

Molenaar, C.M., 1985, Subsurface correlations and depositional history of the Nanushuk Group and related strata, North Slope, Alaska, *in* Huffman, A.C., ed., Geology of the Nanushuk Group and related rocks, North Slope, Alaska: U.S. Geological Survey Bulletin 1614, p. 37–59.

———1988, Depositional history and seismic stratigraphy of Lower Cretaceous rocks in the National Petroleum Reserve in Alaska and adjacent areas, *in* Gryc, George, ed., Geology and exploration of the National Petroleum Reserve in Alaska, 1974 to 1982: U.S. Geological Survey Professional Paper 1399, p. 593–621.

Molenaar, C.M., Bird, K.J., and Kirk, A.R., 1987, Cretaceous and Tertiary stratigraphy of northeastern Alaska, *in* Tailleur, I.L., and Weimer, Paul, eds., Alaskan North Slope geology: Society of Economic Paleontologists and Mineralogists, Pacific Section, and Alaska Geological Society, Book 50, v. 2, p. 513–528.

Moore, T.E., and Box, S.E., 2016, Age, distribution and style of deformation in Alaska north of 60°N: Implications for assembly of Alaska: Tectonophysics, v. 691, p. 133–170. https://doi.org/10.1016/j.tecto.2016.06.025

Moore, T.E., Potter, C.J., O'Sullivan, P.B., Shelton, K.L., and Underwood, M.B., 2004, Two stages of deformation and fluid migration in the west-central Brooks Range fold and thrust belt, northern Alaska, *in* Swennen, Rudy, Roure, François and Granath, J.W., eds., Deformation, fluid flow, and reservoir appraisal in foreland fold and thrust belts: American Association of Petroleum Geologists Hedberg Series, no.1, p. 157–186.

Moore, T.E., Wallace, W.K., Bird, K.J., Karl, S.M., Mull, C.G., and Dillon, J.T., 1994, Geology of northern Alaska, *in* Plafker, George, and Berg, H.C., eds., The Geology of Alaska: The Geology of North America, Geological Society of America, Boulder, Colorado, v. G-1, p. 49–140. https://doi.org/10.1130/DNAG-GNA-G1.49

Mull, C.G., 1979, Nanushuk Group deposition and the late Mesozoic structural evolution of the central and western Brooks Range and Arctic Slope, *in* Ahlbrandt, T.S., ed., Preliminary geologic, petrologic, and paleontologic results of the study of Nanushuk Group rocks, North Slope, Alaska: U.S. Geological Survey Circular 794, p. 5–13.

———1982, The tectonic evolution and structural style of the Brooks Range, Alaska: An illustrated summary, *in* Powers, R.B., ed., Geological studies of the Cordilleran thrust Belt, Volume 1: Rocky Mountain Association of Geologists, p. 1–45.

———1985, Cretaceous tectonics, depositional cycles, and the Nanushuk Group, Brooks Range and Arctic Slope, Alaska, *in* Huffman, A.C., ed., Geology of the Nanushuk Group and related rocks, North Slope, Alaska: U.S. Geological Survey Bulletin 1614, p. 7–36.

Mull, C.G., Glenn, R.K., and Adams, K.E., 1997, Tectonic evolution of the central Brooks Range mountain front: Evidence from the Atigun Gorge region: Journal of Geophysical Research, v. 102, p. 20,749–20,773. http://dx.doi.org/10.1029/96JB03732

Mull, C.G., Harris, E.E., Delaney, P.R., and Swenson, R.F., 2009, Geology of the Cobblestone Creek–May Creek area, east-central Brooks Range Foothills, Alaska: Alaska Division of Geological & Geophysical Surveys Preliminary Interpretive Report 2009-5, 1 sheet, scale 1:63,360, 40 p.

Mull, C.G., Houseknecht, D.W., and Bird, K.J., 2003, Revised Cretaceous and Tertiary stratigraphic nomenclature in the Colville basin, northern Alaska: U.S. Geological Survey Professional Paper 1673, 51 p.

Mull, C.G., Houseknecht, D.W., Pessel, G.H., and Garrity, C.P., 2004, Geologic map of the Umiat Quadrangle, Alaska: U.S. Geological Survey Scientific Investigations Map 2817-A, 1 sheet, scale 1:250,000.

———2005, Geologic map of the Ikpikpuk River Quadrangle, Alaska: U.S. Geological Survey Scientific Investigations Map 2817-B, 1 sheet, scale 1:250,000.

Oldow, J.S., Seidensticker, C.M., Phelps, J.C., Julian, F.E., Gottschalk, R.R., Boler, K.W., Handschy, J.W., and Ave Lallemant, H.G., 1987, Balanced cross sections through the central Brooks Range and North Slope, Arctic Alaska: American Association of Petroleum Geologists, 8 plates, 19 p.

O'Sullivan, P.B., 1996, Late Mesozoic and Cenozoic thermotectonic evolution of the Colville basin, North Slope, Alaska, *in* Johnsson, M.J., and Howell, D.G., eds., Thermal evolution of sedimentary basins in Alaska: U.S. Geological Survey Bulletin 2142, p. 45–79.

O'Sullivan, P.B., Green, P.F., Bergman, S.C., Decker, John, Duddy, I.R., Gleadow, A.J.W., and Turner, D.L., 1993, Multiple phases of Tertiary uplift and erosion in the Arctic National Wildlife Refuge, Alaska, revealed by apatite fission track analysis: American Association of Petroleum Geologists Bulletin, v. 77, p. 359–385.

O'Sullivan, P.B., Murphy, J.M., and Blythe, A.E., 1997, Late Mesozoic and Cenozoic thermotectonic evolution of the central Brooks Range and adjacent North Slope foreland basin, Alaska: Including fission track results from the Trans-Alaska Crustal Transect (TACT): Journal of Geophysical Research, v. 102, p. 20,821–20,845. http://dx.doi.org/10.1029/96JB03411

O'Sullivan, P.B., and Wallace, W.K., 2002, Out-of-sequence, basement-involved structures in the Sadlerochit Mountains region of the Arctic National Wildlife Refuge, Alaska—Evidence and implications from fission-track thermochronology: Geological Society of America Bulletin, v. 114, p. 1,356–1,378. https://doi.org/10.1130/0016-7606(2002)114%3C1356:OOSBIS%3E2.0.CO;2

O'Sullivan, P.B., Wallace, W.K. and Murphy, J.M., 1998, Fission track evidence for apparent out-of-sequence Cenozoic deformation along the Philip Smith Mountain front, northeastern Brooks Range, Alaska: Earth and Planetary Science Letters, v. 164, p. 435–449. https://doi.org/10.1016/S0012-821X(98)00237-4

Peters, K.E., Magoon, L.B., Bird, K.J., Valin, Z.C., and Keller, M.A., 2006, North Slope Alaska: Source-rock distribution, richness, thermal maturity and petroleum charge: American Association of Petroleum Geologists Bulletin, v. 90, p. 261–292. https://doi.org/10.1306/09210505095

Reed, J.C., 1958, Exploration of Naval Petroleum Reserve No. 4 and adjacent areas, northern Alaska, 1944–53; Part 1, History of the exploration: U.S. Geological Survey Professional Paper 301, 2 sheets, scale 1:1,000,000, 192 p.

Reger, R.D., Stevens, D.S.P., Cruse, G.R., and Livingston, H.R., 2003, Survey of geology, geologic materials, and geologic hazards in proposed access corridors in selected quadrangles, Alaska: Alaska Division of Geological & Geophysical Surveys Miscellaneous Publication, 72 p.

Robinson, F.M., 1958, Test wells, Gubik area, Alaska: U.S. Geological Survey Professional Paper 305-C, 2 sheets, p. 207–264.

Sanders, C.M., 2014, Structural geology of the Big Bend anticline, Brooks Range foothills, Alaska: University of Alaska Fairbanks, master's thesis, 153 p.

Schindler, J.F., 1988, History of exploration in the National Petroleum Reserve in Alaska, with emphasis on the period from 1975 to 1982, *in* Gryc, George, ed., Geology and exploration of the National Petroleum Reserve in Alaska, 1974 to 1982: U.S. Geological Survey Professional Paper 1399, p. 13–72.

Schrader, F.C., 1902, Geological section of the Rocky Mountains in northern Alaska: Geological Society of America Bulletin, v. 13, p. 233–252. https://doi.org/10.1130/GSAB-13-233

Schrader, F.C., 1904, A reconnaissance in northern Alaska across the Rocky Mountains, along Koyukuk, John, Anaktuvuk, and Colville rivers and the Arctic Coast to Cape Lisburne, in 1901: U.S. Geological Survey Professional Paper 20, 2 sheets, scale 1:1,250,000, 139 p.

Shimer, Grant, 2013, Sedimentology and stratigraphy of the Nanushuk Formation and related foreland basin deposits, central Brooks Range foothills, Alaska: University of Alaska Fairbanks, Ph.D. dissertation, 165 p.

Shimer, G.T., Benowitz, J.A., Layer, P.W., McCarthy, P.J., Hanks, C.L., and Wartes, M.A., 2016, $^{40}Ar/^{39}Ar$ ages and geochemical characterization of Cretaceous bentonites in the Nanushuk, Seabee, Tuluvak, and Schrader Bluff formations, North Slope, Alaska: Cretaceous Research, v. 57, p. 325–341. https://doi.org/10.1016/j.cretres.2015.04.008

Shimer, G.T., McCarthy, P.J., and Hanks, C.L., 2014, Sedimentology, stratigraphy, and reservoir properties of an unconventional, shallow, frozen petroleum reservoir in the Cretaceous Nanushuk Formation at Umiat Field, North Slope, Alaska: American Association of Petroleum Geologists Bulletin, v. 98, p. 631–661. https://doi.org/10.1306/09031312239

Smith, P.S. and Mertie, J.B., Jr., 1930, Geology and mineral resources of northwestern Alaska: U.S. Geological Survey Bulletin 815, 4 sheets, scale 1:500,000, 351 p.

Stevens, D.S.P., Reger, R.D., and Smith, R.L., 2003, Survey of geology, geologic materials, and geologic hazards in proposed access corridors in the Umiat Quadrangle, Alaska: Alaska Division of Geological & Geophysical Surveys Miscellaneous Publication, 5 sheets, scale 1:250,000.

Sylvester, A.G., 1988, Strike-slip faults: Geological Society of America Bulletin, v. 100, p. 1,666–1,703. https://doi.org/10.1130/0016-7606(1988)100%3C1666:SSF%3E2.3.CO;2

Till, A.B., 1992, Detrital blueschist-facies metamorphic mineral assemblages in Early Cretaceous sediments of the foreland basin of the Brooks Range, Alaska, and implications for orogenic evolution: Tectonics, v. 11, p. 1,207–1,223. http://dx.doi.org/10.1029/92TC01104

Till, A.B., and Snee, L.W., 1995, 40Ar/39Ar evidence that formation of blueschists in continental crust was synchronous with foreland fold and thrust belt deformation, western Brooks Range, Alaska: Journal of Metamorphic Geology, v. 13, p. 41–60. http://dx.doi.org/10.1111/j.1525-1314.1995.tb00204.x

Triezenberg, P.J., Hart, P.E., and Childs, J.R., 2016, National Archive of Marine Seismic Surveys (NAMSS): A USGS data website of marine seismic reflection data within the U.S. Exclusive Economic Zone (EEZ): U.S. Geological Survey Data Release.

Turner, D.L., Forbes, R.B., and Dillon, J.T., 1979 K–Ar geochronology of the southwestern Brooks Range, Alaska: Canadian Journal of Earth Sciences, v. 16, p. 1,789–1,804. https://doi.org/10.1139/e79-164

Twiss, R.J., and Moores, E.M., 1992, Structural Geology: W.H. Freeman and Company, New York, 532 p.

van der Kolk, D.A, 2016, Marine–continental transitions in a greenhouse world: Reconstructing Late Cretaceous deltas of paleopolar Arctic Alaska and Utah: The University of Texas at Austin, Ph.D. dissertation, 297 p.

van der Kolk, D.A., Flaig, P.P., and Hasiotis, S.T., 2015, Paleoenvironmental reconstruction of a Late Cretaceous, muddy, river-dominated polar deltaic system: Schrader Bluff–Prince Creek Formation transition, Shivugak Bluffs, North Slope of Alaska, U.S.A.: Journal of Sedimentary Research, v. 8, p. 903–936. https://doi.org/10.2110/jsr.2015.58

Vogl, J.J., Calvert, A.T., and Gans, P.B., 2002, Mechanisms and timing of exhumation of collision-related metamorphic rocks, southern Brooks Range, Alaska: Insights from 40Ar/39Ar thermochronology: Tectonics, v. 21, p. 2-1–2-17. http://dx.doi.org/10.1029/2000TC001270

Wallace, W.K., 2008, Mechanical stratigraphy and the structural geometry and evolution of the central and eastern foothills of the Brooks Range, northern Alaska, *in* Hanks, C.L., ed., Unraveling the Timing of Fluid Migration and Trap Formation in the Brooks Range Foothills: A Key to Discovering Hydrocarbons: Final Report, prepared for U.S. Department of Energy, National Energy Technology Laboratory (DOE Award Number DE-FC26-06NT41248), p. 2-1–2-34.

Watt, J.S., Huckabay, Allen, and Landt, M.R., 2010, Umiat: A North Slope giant primed for oil development: Oil and Gas Journal, v. 108, issue 1.

Wentz, Raelene, 2014, Fracture characteristics and distribution in Cretaceous rocks near the Umiat anticline, North Slope of Alaska: University of Alaska Fairbanks, master's thesis, 154 p.

Whittington, C.L., 1956, Revised stratigraphic nomenclature of Colville Group, *in* Gryc, George, Bergquist, H.R., Detterman, R.L., Patton, W.W., Jr., Robinson, F.M., Rucker, F.P., and Whittington, C.L., Mesozoic sequence in Colville River region, northern Alaska: American Association of Petroleum Geologists Bulletin, v. 40, no. 2, p. 244–253.

APPENDIX 1

Table A1. List of exploration wells in the Umiat–Gubik area, including uppermost formation picks. These stratigraphic constraints were employed in completing the interpretive geologic mapping. Wells are plotted and labeled on sheet 1. Well data are from the Alaska Oil and Gas Conservation Commission (AOGCC) online databases and Alaska Division of Oil and Gas. K.J. Bird picks are from U.S. Geological Survey (written communication, 2010). Latitude and longitude reported in NAD27. Explanation: Single dash—not applicable; asterisk—discovery well.

Field Name	Well Name	Well Operator	Completion Date	Latitude	Longitude	Uppermost Formation Pick	Measured Depth (feet)	Pick Source	Comment (this study)	Interpretation (this study)
Umiat oil field	Umiat Test No. 1	U.S. Navy	10/05/1946	69.396529	-152.329178	Seabee	9–915	K.J. Bird	–	Seabee at surface
	Umiat Test No. 2	U.S. Navy	12/12/1947	69.384463	-152.083611	Nanushuk	80–1060	K.J. Bird	Quaternary: 9–80' (Collins, 1958)	Nanushuk near surface
	Umiat Test No. 3*	U.S. Navy	12/26/1946	69.387807	-152.087284	Nanushuk	60-total depth	K.J. Bird	not sampled: 9–60' (Collins, 1958); total depth at 572' in Kn (Collins, 1958)	Nanushuk near surface
	Umiat Test No. 4	U.S. Department of Interior	07/29/1950	69.388905	-152.081419	Nanushuk	90-total depth	K.J. Bird	not sampled: 1–90' (Collins; 1958); total depth at 840' in Kn (Collins, 1958)	Nanushuk near surface
	Umiat Test No. 5	U.S. Department of Interior	10/4/1951	69.384739	-152.082264	Nanushuk	65–1060	Collins (1958)	not sampled: 0–65' (Collins, 1958); probably spudded in Kn (Collins, 1958)	Nanushuk near surface
	Umiat Test No. 6	U.S. Navy	12/12/1950	69.378915	-152.094441	Seabee	30–220	K.J. Bird	not sampled: 3–100' (Collins, 1958); top of Ks at 31' (Collins, 1958)	Seabee near surface
	Umiat Test No. 7	U.S. Navy	04/12/1951	69.375850	-152.104716	Seabee	50–380	K.J. Bird	Quaternary: 4–50' (Collins, 1958)	Seabee near surface
	Umiat Test No. 8	U.S. Department of Interior	08/28/1951	69.399748	-152.115565	Seabee	20–60	K.J. Bird	Quaternary: 5–20' (Collins, 1958)	Seabee near surface
	Umiat Test No. 9	U.S. Navy	01/15/1952	69.387244	-152.169749	Nanushuk	6–1090	K.J. Bird; Collins (1958)	–	Nanushuk at surface
	Umiat Test No. 10	U.S. Navy	01/10/1952	69.401132	-152.132500	Nanushuk	5–250	K.J. Bird	Nanushuk thrusted over Seabee at 250'	Nanushuk near surface
	Umiat Test No. 11	U.S. Navy	08/29/1952	69.408078	-152.099460	Tuluvak	22–775	K.J. Bird	–	Tuluvak near surface
	Seabee Test No. 1	Husky Oil NPR Operations, Inc.	04/15/1980	69.380167	-152.175404	Seabee	100–280	K.J. Bird	–	Seabee near surface
	Umiat No. 18	Linc Energy Operations, Inc.	4/29/2013	69.384851	-152.119386	Nanushuk	230–1038	Well Completion or Recompletion Report and Log (AOGCC)	–	Nanushuk near surface
	Umiat No. 23H	Linc Energy Operations, Inc.	3/20/2014	69.394405	-152.196331	–	–	–	well deviated to horizontal	Seabee near surface
Gubik gas field	Gubik Test No. 1*	U.S. Navy	8/11/1951	69.433907	-151.475830	Schrader Bluff (Barrow Trail Member)	67–295	Robinson (1958)	Pliocene to Recent: 12-67' (Robinson, 1958)	Barrow Trail near surface
	Gubik Test No. 2	U.S. Navy	12/14/1951	69.424191	-151.441676	Schrader Bluff (Barrow Trail Member)	160–555	Robinson (1958)	no core or cuttings from 12–160' (Robinson, 1958)	Barrow Trail near surface
	Gubik Unit No. 1	Colorado Oil and Gas	11/12/1963	69.428979	-151.413502	Schrader Bluff	110–1136	K.J. Bird	Schrader Bluff members not picked	Barrow Trail near surface
	Gubik No. 3	Anadarko Petroleum Corporation	4/14/2008	69.441454	-151.442073	Tuluvak	1079–?	Well Completion or Recompletion Report and Log (AOGCC)	Schrader Bluff not designated; top Seabee not picked	Barrow Trail near surface
	Gubik No. 4	Anadarko Petroleum Corporation	4/6/2009	69.429660	-151.293870	Tuluvak	1461–2315	Well Completion or Recompletion Report and Log (AOGCC)	Schrader Bluff not designated; top Seabee not picked	Sentinel Hill near surface
East Umiat gas field	East Umiat Unit No. 1*	Devon Energy Production Corporation LP	3/28/1964	69.344871	-151.743740	Tuluvak	17–510	K.J. Bird	–	Tuluvak near surface
	East Umiat Unit No. 2	McCulloch Oil Co	5/21/1969	69.359128	-151.861659	Tuluvak	12–?	K.J. Bird	top Seabee not picked	Tuluvak near surface
	Colville Unit No. 1	McCulloch Oil Co	3/11/1970	69.337493	-151.912631	Prince Creek/ Schrader Bluff	23–?	K.J. Bird	top Tuluvak not picked	–
						Seabee	1640–2950	K.J. Bird	uppermost formation pick that provides stratigraphic context	Rogers Creek near surface
	Colville Unit No. 2	McCulloch Oil Co	12/25/1971	69.365277	-151.833690	Tuluvak	23–?	K.J. Bird	top Seabee not picked	Tuluvak near surface
	Chandler No. 1	Anadarko Petroleum Corporation	4/4/2009	69.355210	-151.633409	Tuluvak	120–1070	Well Completion or Recompletion Report and Log (AOGCC)	–	Rogers Creek near surface

APPENDIX 2

Table A2. Spreadsheet of fracture data employed in the Colville River corridor structural analysis of this study. Shear fractures are in bold; shear fractures that are uniquely constrained kinematically are in bold and underlined. See text for stereonet plots and discussion. Latitude and longitude reported in NAD27.

	Locality	Map Unit	Station	Latitude	Longitude	Dip Azimuth	Dip	Rake	Rake Direction	Comment
1	Colville incision	Nanushuk Formation	11BG304	69.272584	152.585510	265	84			
2			11BG305 (traverse)	69.273844	152.610218	165	73			
3						84	89			
4						170	75			
5						159	54			
6						175	50			
7						176	54			
8						183	55			
9						165	54			
10						78	83			
11						88	86			
12						87	90			
13						166	44			
14						163	69			
15						62	77			
16						174	63			
17						78	86			
18						171	64			
19						282	80			
20						274	84			
21						172	63			
22						176	57			
23						92	88			
24						110	54			
25						**103**	**84**	27	SW	Reverse, left lateral
26						101	84			
27						102	86			
28						272	88			
29						**102**	**89**	46	SW	Reverse, left lateral
30						98	89			
31						276	86			
32						155	49			
33						**256**	**76**	30	S	Reverse, right lateral
34						257	82			
35						108	82			
36						69	89			
37						**105**	**72**	15	SW	Reverse, left lateral
38						81	74			
39						**56**	**86**	23	SE	Normal, right lateral
40						175	52			
41						**246**	**78**	29	NW	Normal, right lateral
42						279	82			
43						291	89			
44						**250**	**77**	34	NW	Normal, right lateral
45						171	46			
46						242	71			
47						173	66			
48						250	72			
49						174	61			
50						252	81			
51						178	60			
52						171	48			
53						166	57			
54						172	68			
55						187	60			
56						185	61			
57						170	55			
58						184	61			
59						175	57			
60						199	67			

Table A2, continued. Spreadsheet of fracture data employed in the Colville River corridor structural analysis of this study. Shear fractures are in bold; shear fractures that are uniquely constrained kinematically are in bold and underlined. See text for stereonet plots and discussion. Latitude and longitude reported in NAD27.

	Locality	Map Unit	Station	Latitude	Longitude	Dip Azimuth	Dip	Rake	Rake Direction	Comment
61	Fossil Creek bluff	Schrader Bluff Formation, Barrow Trail Member	11TMH297	69.301093	152.372929	198	83			
62						208	73			
63						224	85			
64						206	77			
65						261	87			
66						266	88			
67						208	79			
68						195	72			
69						202	76			
70						206	76			
71						264	87			
72						200	79			
73						261	89			
74						214	76			
75						199	82			
76						213	82			
77						204	69			
78						210	72			
79						203	79			
80						214	67			
81						274	87			
82						211	78			
83						205	74			
84						200	69			
85						103	65			
86						207	68			
87						267	81			
88						277	88			
89						**202**	**74**			Shear fracture
90						202	76			
91						**180**	**82**			Shear fracture
92						277	74			
93						212	68			
94						206	75			
95						95	88			
96						100	86			
97						**190**	**77**			Shear fracture
98						**187**	**77**			Shear fracture
99						216	78			
100						190	84			
101						**204**	**68**			Shear fracture
102						201	84			
103						297	86			
104						114	82			
105						195	78			
106						199	80			
107						281	89			
108						198	69			
109						197	81			
110						210	74			
111						102	88			
112						210	68			
113						276	89			
114						205	79			
115						276	89			
116						203	72			
117						277	88			
118						106	85			
119						206	74			
120						111	85			

Table A2, continued. Spreadsheet of fracture data employed in the Colville River corridor structural analysis of this study. Shear fractures are in bold; shear fractures that are uniquely constrained kinematically are in bold and underlined. See text for stereonet plots and discussion. Latitude and longitude reported in NAD27.

	Locality	Map Unit	Station	Latitude	Longitude	Dip Azimuth	Dip	Rake	Rake Direction	Comment
121	Tattitgak Bluff, west	Schrader Bluff Formation, Barrow Trail Member	11BG261	69.333392	152.255174	295	85			
122	Tattitgak Bluff, west	Schrader Bluff Formation, Barrow Trail Member	11BG260	69.334172	152.254704	**134**	**12**	22	SW	Normal, right lateral
123						**185**	**42**	86	NW	Reverse, left lateral
124						**321**	**14**	25	NE	
125						297	70			
126						**52**	**66**	30	SE	Normal, right lateral
127						**29**	**33**	57	NW	
128						**107**	**88**			Left lateral
129						**326**	**16**	57	NE	Reverse, left lateral
130						**151**	**31**	72	SW	Reverse, left lateral
131						**198**	**27**	87	SE	Reverse, right lateral
132						**54**	**44**	47	NW	Reverse, right lateral
133						**355**	**15**	87	SW	
134						**182**	**23**	84	SE	Reverse, right lateral
135	Tattitgak Bluff, west	Schrader Bluff Formation, Barrow Trail Member	11BG259	69.335102	152.253404	72	86			
136						280	84			
137						**354**	**21**	86	W	Reverse, right lateral
138						176	78			
139						108	88			
140						275	74			
141						**1**	**34**	65	W	Reverse, right lateral
142						105	88			
143						**335**	**23**	75	NE	Reverse, left lateral
144						**325**	**18**	65	NE	
145						**163**	**19**	85	NE	
146						**139**	**31**	80	SW	
147						**325**	**18**			Reverse
148						**198**	**18**	84	SE	Reverse, right lateral
149	Tattitgak Bluff, west	Schrader Bluff Formation, Barrow Trail Member	11TMH230	69.335812	152.252294	182	89			
150						266	76			
151						4	86			
152						24	77			
153						196	82			
154						27	77			
155						291	89			
156						111	84			
157						9	81			
158						4	79			
159						193	80			
160						7	84			
161						282	76			
162						102	89			
163						359	73			
164						3	86			
165						25	75			
166						1	82			
167						197	85			
168						359	85			
169						10	80			
170						1	80			
171						10	87			
172	Tattitgak Bluff, west	Schrader Bluff Formation, Barrow Trail Member	11BG258	69.336052	152.251844	326	79			
173						0	88			
174						9	85			
175						332	84			
176						14	75			
177						2	72			
178						8	86			
179						5	89			
180						12	88			
181						356	81			
182						188	82			
183						193	88			

Table A2, continued. Spreadsheet of fracture data employed in the Colville River corridor structural analysis of this study. Shear fractures are in bold; shear fractures that are uniquely constrained kinematically are in bold and underlined. See text for stereonet plots and discussion. Latitude and longitude reported in NAD27.

	Locality	Map Unit	Station	Latitude	Longitude	Dip Azimuth	Dip	Rake	Rake Direction	Comment
184	Tattitgak Bluff, west	Schrader Bluff Formation, Barrow Trail Member	11BG257	69.337042	152.249384	0	90			
185						15	79			
186						18	76			
187						357	84			
188						10	87			
189						17	69			
190						14	72			
191	Tattitgak Bluff, west	Schrader Bluff Formation, Barrow Trail Member	11BG239	69.338072	152.243624	**4**	**87**			Right lateral
192						15	81			
193						13	87			
194						8	82			
195						10	86			
196						359	88			
197						30	79			
198						19	76			
199						12	84			
200						17	75			
201						14	74			
202	Tattitgak Bluff, east	Schrader Bluff Formation, Barrow Trail Member	11DJM289	69.337022	152.173097	57	87			
203						310	87			
204						120	83			
205						118	85			
206						62	81			
207						57	81			
208						50	87			
209						322	87			
210						66	80			
211						240	81			
212						355	52			
213						0	48			
214						237	89			
215						3	55			
216						0	47			
217						352	53			
218						17	52			
219						65	82			
220						352	52			
221						351	51			
222						55	87			
223						60	85			
224						116	85			
225						302	85			
226						48	81			
227						50	75			
228						304	85			
229						17	73			
230						350	40			
231						350	42			
232						45	82			
233						58	86			
234						352	54			
235						326	86			
236						60	82			
237						322	87			
238						54	70			
239						45	83			
240						320	87			
241						48	81			
242						47	89			
243						334	79			
244						48	85			
245						354	50			
246						9	54			
247						1	47			
248						319	70			
249						348	55			
250						353	43			
251						50	87			

Table A2, continued. Spreadsheet of fracture data employed in the Colville River corridor structural analysis of this study. Shear fractures are in bold; shear fractures that are uniquely constrained kinematically are in bold and underlined. See text for stereonet plots and discussion. Latitude and longitude reported in NAD27.

	Locality	Map Unit	Station	Latitude	Longitude	Dip Azimuth	Dip	Rake	Rake Direction	Comment
252	Umiat Mountain, west	Nanushuk Formation	11BG306	69.388100	152.023674	156	71			
253						157	72			
254						155	70			
255						157	67			
256						156	62			
257						164	62			
258						159	56			
259						161	59			
260						172	55			
261						164	57			
262						162	52			
263						157	64			
264						158	63			
265						162	40			
266						161	45			

Table A2, continued. Spreadsheet of fracture data employed in the Colville River corridor structural analysis of this study. Shear fractures are in bold; shear fractures that are uniquely constrained kinematically are in bold and underlined. See text for stereonet plots and discussion. Latitude and longitude reported in NAD27.

	Locality	Map Unit	Station	Latitude	Longitude	Dip Azimuth	Dip	Rake	Rake Direction	Comment
267	Umiat Mountain, east	Seabee Formation	11BG308	69.387980	151.985485	251	78			
268						182	88			
269						262	88			
270						254	64			
271						182	88			
272						245	66			
273						165	82			
274						254	82			
275						264	65			
276						248	82			
277						170	80			
278						240	75			
279						236	80			
280						163	73			
281						240	79			
282						140	87			
283						138	89			
284						246	75			
285						235	82			
286						344	82			
287						330	85			
288						233	75			
289						132	78			
290						330	80			
291						241	74			
292						240	76			
293						237	77			
294						232	76			
295						237	76			
296						241	81			
297						235	78			
298						237	80			
299						236	78			
300						247	73			
301						249	79			
302						194	79			
303						179	81			
304						165	83			
305						165	82			
306						345	83			
307						135	80			
308						232	71			
309						242	79			
310						243	83			
311						158	80			
312						240	79			
313						157	84			
314						155	73			
315						156	85			
316						156	81			
317						242	71			
318						162	86			
319						158	84			
320						142	81			
321						164	70			
322						239	83			
323						235	77			
324						241	72			
325						243	57			
326						240	87			

Table A2, continued. Spreadsheet of fracture data employed in the Colville River corridor structural analysis of this study. Shear fractures are in bold; shear fractures that are uniquely constrained kinematically are in bold and underlined. See text for stereonet plots and discussion. Latitude and longitude reported in NAD27.

	Locality	Map Unit	Station	Latitude	Longitude	Dip Azimuth	Dip	Rake	Rake Direction	Comment
327	Umiat Mountain, east	Tuluvak Formation	11DJM291	69.385780	151.977516	**242**	**72**			Left lateral
328						242	85			
329						169	77			
330						**245**	**73**			Left lateral
331						178	89			
332						265	78			
333						**303**	**77**			Left lateral
334						180	88			
335						242	81			
336						68	87			
337						183	77			
338						245	89			
339						26	87			
340						249	87			
341						302	72			
342	Umiat Mountain, east	Tuluvak Formation	11TMH299	69.385530	151.976836	243	89			
343						240	89			
344						70	84			
345						245	86			
346						71	85			
347						296	82			
348						297	75			
349						242	82			
350						294	70			
351						302	89			
352						238	87			
353						15	86			
354						17	83			
355						198	80			
356						241	74			
357						**249**	**78**	1	SE	Reverse, right lateral
358						**288**	**76**	2	SW	Normal, left lateral
359						**303**	**83**	0	NE	Right lateral
360	Umiat Mountain, east	Tuluvak Formation	11BG309	69.385480	151.975706	244	90			
361						30	80			
362						298	77			
363						251	85			
364						298	80			
365						294	78			
366						242	90			
367						248	88			
368						250	84			
369						252	85			
370						179	89			
371						**240**	**85**	5	NW	Normal, right lateral
372						226	76			
373						197	88			
374						180	89			
375						177	89			
376						62	85			
377						139	77			
378						240	90			
379						235	82			
380						243	76			
381						175	88			
382						191	90			
383						190	74			

Table A2, continued. Spreadsheet of fracture data employed in the Colville River corridor structural analysis of this study. Shear fractures are in bold; shear fractures that are uniquely constrained kinematically are in bold and underlined. See text for stereonet plots and discussion. Latitude and longitude reported in NAD27.

	Locality	Map Unit	Station	Latitude	Longitude	Dip Azimuth	Dip	Rake	Rake Direction	Comment
384	Shivugak Bluff, west	Schrader Bluff Formation, Barrow Trail Member	11DJM290	69.406549	151.845481	195	81			
385						117	88			
386						10	89			
387						130	73			
388						200	75			
389						225	78			
390						170	68			
391						197	67			
392						105	90			
393						183	73			
394						285	78			
395						123	77			
396						175	82			
397						115	85			
398						193	45			
399						190	42			
400						178	42			
401						188	85			
402						155	45			
403						126	68			
404						158	40			
405						193	89			
406						192	89			
407						284	87			
408						122	71			
409						15	85			
410						320	89			
411						21	89			
412						12	89			
413						15	85			
414						122	80			
415						355	77			
416						290	82			
417						132	45			
418						175	80			
419						10	80			
420						168	59			
421						103	86			
422						91	81			
423						274	82			
424						7	81			
425						12	60			
426						193	77			
427						103	58			
428						190	85			
429						184	60			
430						140	71			
431						190	70			
432						69	72			
433						109	88			

Table A2, continued. Spreadsheet of fracture data employed in the Colville River corridor structural analysis of this study. Shear fractures are in bold; shear fractures that are uniquely constrained kinematically are in bold and underlined. See text for stereonet plots and discussion. Latitude and longitude reported in NAD27.

	Locality	Map Unit	Station	Latitude	Longitude	Dip Azimuth	Dip	Rake	Rake Direction	Comment
434	Shivugak Bluff, east	Prince Creek Formation	11TMH298	69.428899	151.607012	158	83			
435						158	85			
436						120	89			
437						356	88			
438						106	79			
439						105	89			
440						161	79			
441						106	71			
442						191	85			
443						50	87			
444						112	89			
445						228	89			
446						71	85			
447						125	84			
448						252	86			
449						259	88			
450						218	61			
451						209	77			
452						118	79			
453						251	82			
454						122	78			
455						126	86			
456						55	76			
457						144	88			
458						246	88			
459						146	89			
460						255	87			
461						6	82			
462						71	81			
463						104	52			
464						30	82			
465						197	80			
466						230	78			
467						297	87			
468						113	77			
469						163	74			
470						291	87			
471						80	87			
472						72	85			
473						118	86			
474						334	87			
475						220	85			
476						117	79			
477						213	88			
478						36	75			
479						56	76			
480						114	72			
481						295	89			
482						118	70			
483						67	85			
484						107	83			
485						258	85			
486						14	82			
487						128	83			
488						66	85			
489						112	85			
490						176	85			
491						114	82			
492						246	82			
493						73	88			